Metabolic syndrome, olfactory dysfunction, and brain morphology

Dissertation

zur Erlangung des Doktorgrades (MD/PhD)

der Hohen Medizinischen Fakultät

der Rheinischen Friedrich-Wilhelms-Universität

Bonn

Ran Lu

aus Hubei, China

2019

Angefertigt mit der Genehmigung

der Medizinischen Fakultät der Universität Bonn

1. Gutachter: Prof. Dr. Dr. Monique M. B. Breteler
2. Gutachter: Prof. Dr. Aad van der Lugt

Tag der Mündlichen Prüfung: August 28, 2019

Aus der Populationsbezogene Gesundheitsforschung, Deutsches Zentrum für Neurodegenerative Erkrankungen e. V.

Direktorin: Prof. Dr. Dr. Monique M.B. Breteler

Table of Contents

Manuscripts based on the studies described in this thesis:

Chapter 2

Santiago Estrada*; Ran Lu*;…; Martin Reuter, Monique M.B. Breteler. (To be submitted)

Chapter 3

Ran Lu; N. Ahmad Aziz;…; Martin Reuter; Monique M.B. Breteler. (To be submitted)

Chapter 4

Ran Lu; N. Ahmad Aziz; Martin Reuter; Tony Stöcker; Monique M.B. Breteler. Disentangling the structural components of olfactory dysfunction in the general population. (Submitted)

Chapter 5

Ran Lu; N. Ahmad Aziz; Kersten Diers; Tony Stöcker; Martin Reuter; Monique M.B. Breteler. Insulin resistance accounts for metabolic syndrome-related alterations in brain structure. (Submitted)

Abbreviations

ATP	Adenosine triphosphate
BP	Blood pressure
CI	Confident interval
eTIV	the Estimated Total Intracranial Volume
DSC	Dice similarity coefficient
FDR	False discovery rate
FPG	Fasting plasma glucose
FSI	Fasting serum insulin
GMV	Gray matter volume
HDL-C	High-density lipoprotein cholesterol
HOMA-IR	Homeostasis model assessment of insulin resistance
ICC	Intraclass correlation coefficient
ICH-GCP	International Conference on Harmonisation Good Clinical Practice standards
LDL-C	Low-density lipoprotein cholesterol
MetS	Metabolic syndrome
MPRAGE	Magnetization-prepared rapid gradient-echo
MRI	Magnetic resonance imaging
N	Number

NCEP ATP	National Cholesterol Education Program Adult Treatment Panel
OBV	Olfactory bulb volume
Rx	Pharmacologic treatment
SD	Standard deviation
SIT-12	12-item “Sniffin’ Sticks” odor identification test
SPACE	Sampling perfection with application-optimized contrasts by using flip angle evolution
TBV	Total brain volume
TC	Total cholesterol
WMV	White matter volume

1. Introduction

1.1 Metabolic syndrome and olfactory dysfunction

Both metabolic syndrome (MetS) and olfactory dysfunction are highly prevalent disorders. MetS, a clustering of metabolic components, including abdominal obesity, elevated glucose and blood pressure levels, as well as dyslipidemia (i.e. low high-density lipoprotein cholesterol [HDL-C] and hypertriglyceridemia), is a major public health burden worldwide.[1] Olfactory dysfunction, defined as an absent or reduced sense of smell, could affect up to one-fourth of the general population.[2]

In the past decades, several individual components of MetS, i.e. obesity, hypertension, and hyperglycemia, have been found to be associated with olfactory dysfunction.[3,4] Consequently, it has been suggested that metabolic disturbance could perturb olfactory physiology and function. A link between olfaction and metabolic status and circulating endocrine molecules is corroborated by a wide range of animal studies.[5-8] However, the association between MetS, as a group of several metabolic disorders, and olfactory dysfunction has only been evaluated recently in the general human population: Two studies based on data from the Korean national survey demonstrated that individuals with MetS more frequently reported olfactory dysfunction compared to those without MetS.[9,10] Olfactory dysfunction is an often neglected condition, and less than a quarter of individuals with smell dysfunction are aware of the impairment until formally tested.[11] Therefore, olfactory self-assessment is not a reliable measure to assess olfactory function compared to objective psychophysical tests.[12] To date, it remains unclear how objectively assessed olfactory function is associated with MetS in the general population.

1.2 Olfactory function and metabolic syndrome: their link to the brain

Olfactory dysfunction and MetS have both been closely linked with loss of brain function and neurodegeneration. Accumulating evidence suggests that olfactory impairment is a prodromal symptom of many neurological and neurodegenerative disorders, including

Alzheimer's disease and Parkinson's disease.[11,13,14] It has also been proposed as a preclinical marker for cognitive impairment and a predictor of cognitive decline.[15-18] Similarly, an increased risk of cognitive impairment and dementia was observed in participants with MetS and its components in both cross-sectional and longitudinal studies.[19-22] Moreover, insulin resistance, as the central physiopathogenesis of MetS,[23] predicted a worse cognitive performance later in life.[19-21] Although the fact that metabolic syndrome and olfactory function are associated with brain function is therefore well established, the structural basis of these associations is not clear.

Normal olfaction requires a functional olfactory pathway involving several brain structures.[24] The odorants are first detected by the olfactory sensory neurons in the upper nasal cavity and transduced into action potentials.[25] The information from the activated neurons is then transmitted along the axons to the olfactory bulb, and further directed to the primary olfactory cortex, which mainly consists of the olfactory tubercle, piriform cortex, entorhinal cortex, amygdala, and parahippocampus. From the primary olfactory cortex, the signals project further to several brain regions, including hippocampus, insula and orbitofrontal cortex.[24] The latter is also called secondary olfactory cortex.

A non-invasive and reliable assessment of brain olfactory structures in humans has become possible with the development of magnetic resonance imaging (MRI). However, to date, there is still limited evidence on the relation between olfactory function and its neuroanatomical correlates. The few studies that reported on the relation between were mostly small-scale studies, enrolling patients with olfactory disorders, such as chronic rhinosinusitis, parosmia, anosmia or congenital olfactory impairment.[26-30] They reported that patients with impaired olfactory function had reduced volumes of several odor-related brain structures, especially olfactory bulb and orbitofrontal cortex, compared to healthy controls. A few clinic-based studies in healthy volunteers, also reported a positive correlation of the volumes of olfactory bulb and orbitofrontal cortex with olfactory function.[31-33] A recent population-based study found additional brain structures, notably smaller volumes of entorhinal cortex, hippocampus, as well as several other mesial temporal lobe structures, to be related with impaired olfaction.[16] However, this study only

included 380 dementia-free elderly with a mean age of 78 years. Therefore, it is unknown if this relationship is present in younger populations.

Compared to olfactory function, the link of MetS with brain structure has received more attention in the literature. A number of studies have examined the effects of individual components of MetS on brain structures (see **Table 1.1**), and showed that indicators of worse metabolic status were associated with smaller total brain volume (TBV) and global and several regional gray matter volumes (GMV), while mixed results were found for the association with white matter volume (WMV).

Table 1.1 Summary of effects of MetS components on brain structures

	(Central) Obesity[a]	Glucose disturbance	Increased blood pressure	Dyslipidemia
TBV	TBV↓[34-36]	TBV↓[37-40]	TBV↓[41,42]	HDL-C↑ TBV↑[43]
WMV	WMV↑[44] , ↓[45], or →[36]	WMV↓[38,46,47] or →[48,49]	WMV→[50]	HDL-C↑ WMV→[51]
GMV				
- global	GMV↓[34,36,45,52]	GMV↓[37,38,47,53,54] mean cortical thickness↓[55]	GMV↓[42]	TC↑ GMV↓[56] LDL-C↑ GMV↓[56] HDL-C↑ cortical thickness↓[57]
- regional	(pre)frontal↓[36,44,45,52,58,59] temporal↓[45,59] insula↓[58,59] amygdala↓[58,59] cingulate↓[45,58] parahippocampus, hippocampus or medial temporal lobe→[34] or ↓[44,45,52,58,60]	(pre)frontal↓[47,54] temporal↓[47,49] cingulate↓[47,54] no difference, or smaller volumes of parahippocampus, hippocampus or medial temporal lobe →[48] or ↓[47,55,61,62]	(pre)frontal↓[50,63,64] parahippocampus, hippocampus or medial temporal lobe→[41,62] or ↓[46,60-62]	HDL-C↑ parahippocampus and temporal cortex↑[51] HDL-C↑ hippocampus →[51,65] or ↑[43]

Abbreviation: TBV, total brain volume; WMV, white matter volume; GMV, gray matter volume; HDL-C, high-density lipoprotein cholesterol; TC, total cholesterol; LDL-C, low-density lipoprotein cholesterol.

[a] (Central) obesity were assessed by waist circumference, waist-to-hip ratio or body mass index.

Given that metabolic disturbances co-occur frequently, considering MetS as a complex entity may be essential to gaining a better understanding of its effects on brain structures. MetS and insulin resistance have been linked with brain structural changes in MRI studies. However, most of these studies were conducted with patients in a clinical setting and focused primarily on cerebral micro- or macro-vascular changes, i.e. white matter hyperintensities, lacunes, or stroke.[66-68] Hence, the number of studies assessing brain morphology in relation to MetS and insulin resistance in the general population is limited. In addition, most of such studies either included only one or two MRI global indices of brain structures such as TBV, GMV, WMV, ventricular fraction, and brain parenchymal fraction,[40,69-71] or showed an exclusive interest in the medial temporal lobe, especially the hippocampus.[40,61] To date, a few cohort studies used voxel-wise morphometry and found that higher insulin resistance or having MetS was associated with either less GMV or progressive gray matter atrophy in several brain regions, especially middle and superior temporal cortices.[72-74] However, those studies were performed in relatively small groups of individuals, usually confined to a restricted age range. Therefore, there is a knowledge gap on the specific regional brain structural alterations in MetS and insulin resistance in the general adult population. Furthermore, it is still unclear whether and to what extent insulin resistance, as a central feature of MetS,[23] underlies the effects of MetS on brain structure.

1.3 Insulin: linking metabolic syndrome with olfactory dysfunction

MetS has been linked to olfactory dysfunction, yet the underlying mechanisms remain unclear. Given that insulin is involved in both olfaction and MetS, the question arises as to whether insulin and its pathological condition, insulin resistance, could offer a potential explanation. In the following, I will first introduce insulin and its major peripheral metabolic functions, and then focus on central insulin and discuss its link to olfactory function and MetS.

Insulin, a peptide produced by β-cells of the pancreas, is a major anabolic hormone regulating the homeostasis of carbohydrates, lipids and proteins. It facilitates glucose uptake, while inhibiting gluconeogenesis and glycogenolysis in the liver and skeletal

muscle.[75] In adipocytes, insulin promotes the uptake of triglyceride from the blood, stimulates the synthesis of fatty acid and triglyceride, and suppresses the rate of lipolysis. It also regulates protein metabolism by increasing the amino acid uptake and protein synthesis.[76] Therefore, impaired function of the insulin under insulin-resistant condition, could induce hyperglycemia and subsequent hyperinsulinaemia,[77] vascular disturbance,[78,79] dyslipidemia and ectopic lipid deposition,[80] and a chronic inflammatory state,[81] thereby contributing to the development of MetS.

The central function of insulin has been recognized only since the ninety seventies and has not yet been fully characterized.[82] The brain is an insulin-sensitive organ. Peripheral insulin, as the main source of central insulin, crosses the blood-brain barrier via a saturable transport system - the brain insulin receptor.[83] Brain insulin receptors are widely, though unevenly distributed in the brain, and are mainly located in regions along the olfactory pathway.[84,85]

The spatial overlap between insulin receptors and brain olfactory structures suggested a link between central insulin and olfaction. Subsequent studies found that the delivery of insulin after intranasal administration follows the olfactory nerves to the olfactory bulb, and accumulates in the brain.[86,87] In animal studies, it was found that central insulin signaling decreased odorant-induced electro-physiological activity in olfactory sensory neurons and modulated the ion channels in the olfactory bulb.[7,88] Several studies in humans likewise found an impaired olfactory sensitivity after peripheral or intranasal insulin administration.[89,90]

Brain insulin plays a pivotal role in the maintenance of metabolic homeostasis. The insulin receptor signaling in the hypothalamus regulates the peripheral metabolic homeostasis by suppressing hepatic glucose production,[91] promoting adipose tissue expansion,[92] and reducing appetite.[93] Brain insulin resistance, which is usually manifested in MetS as a reduced level of insulin receptor binding and impaired responsiveness to insulin stimulation,[94,95] impairs this homeostasis regulation and contributes to energy deficiency, adipose redistribution and impaired control of food intake. The resulting deteriorated peripheral metabolic condition will further impact insulin transport to the central nervous system.[96,97] Moreover, impaired glucose

metabolism and reduced adenosine triphosphate (ATP) production under insulin resistance adversely affect all ATP-dependent processes in the brain, including cellular homeostasis, membrane permeability, synaptic maintenance and remodeling,[98] and thus potentially influence olfactory function.

Therefore, I hypothesized that MetS, and in particular insulin resistance, could lead to olfactory dysfunction, possibly through an effect on olfaction-related brain structures.

1.4 The Rhineland Study

The Rhineland study is an ongoing community-based prospective cohort that started recruitment in March 2016. It enrolls participants aged 30 years and above at baseline from two geographically defined areas in Bonn, Germany.[99] Ethical approval of the study was obtained from the ethics committee of the University of Bonn, Medical Faculty. The study is carried out in accordance with the recommendations of the International Conference on Harmonisation Good Clinical Practice (ICH-GCP) standards. Written informed consent is obtained from each participant in accordance with the Declaration of Helsinki.

All participants enrolled in the study undergo a comprehensive protocol including extensive structural and functional brain imaging, detailed metabolic assessments, as well as olfactory function testing. This allows for the investigation of the relations between MetS, olfactory function and brain morphology.

Brain imaging

The MRI scans are collected on 3T Siemens MAGNETOM Prisma MRI scanners (Siemens Healthcare, Erlangen, Germany) equipped with a 80 mT/m gradient system and a 64-channel head-neck coil.

The standardized acquisition protocol includes a three-dimensional T1-weighted magnetization-prepared rapid gradient-echo (MPRAGE) sequence (acquisition time = 6.5 min, repetition time = 2560 ms, inversion time = 1100 ms, flip angle = 7°, field of view = 256×256 mm, voxel size = 0.8×0.8×0.8 mm^3, 224 sagittal slices), [100,101] and a T2-

weighted sequence using a sampling perfection with application-optimized contrasts by using flip angle evolution (SPACE, repetition time = 2800 ms, echo time = 405 ms, field of view = 256×256 mm, voxel size = 0.8×0.8×0.8 mm^3).

Cortical reconstruction and volumetric segmentation are performed on T1-weighted images using FreeSurfer version 6.0 (http://surfer.nmr.mgh.harvard.edu/). The volumes of subfields of the hippocampus are obtained using a separate processing pipeline implemented in FreeSurfer based on both T1- and T2-weighted scans.[102]

Assessment of metabolic status

Blood samples are collected after an at least 8-hour fast. Fasting serum insulin (FSI), triglyceride and HDL-C are measured using standard protocol in the central lab of University Hospital of Bonn. Fasting plasma glucose (FPG) concentration is measured on the Nightingale platform (Nightingale Health, Helsinki, Finland).[103] Homeostatic assessment of insulin resistance (HOMA-IR) is calculated on the basis of fasting values of glucose and insulin as HOMA-IR = fasting glucose in mmol/L × fasting insulin in mIU/L / 22.5.[104] Waist circumference is measured in underwear with a flexible anthropometric tape (SECA 201) to the nearest millimeter at the midpoint between the last rib and iliac crest. Blood pressure is measured three times over half an hour with an oscillometric blood pressure device (OMRON 705 IT) in a semi-recumbent position, and the average of the second and third measurements is calculated. Participants provide information regarding any anti-diabetic, anti-hypertensive and lipid-modifying medications used currently and in the past 12 months.

Olfactory function measurement

Olfactory function is assessed by 12-item “Sniffin’ Sticks” odor identification test (SIT-12).[105] Participants are presented each of twelve felt-tip sticks from the test kit (Burghart Messtechnik GmbH, Germany) approximately 2 cm from their nose for 3 to 4 seconds with an at least 20-second interval, and they have to choose one of the four answer options for each odorant. The sum of the correct responses is calculated as the final score (range: 0-12).

Self-reported nasal patency is recorded as “blocked” or “free” and is used as an indicator of general nasal condition.

1.5 Objectives

The overall goal of my research was to elucidate the relations between metabolic syndrome, brain structure, in particular olfactory brain structures, and olfactory function (**Figure 1.1**). Specifically, I aimed to

1. Assess the association of MetS and insulin resistance with olfactory structures and function.

2. Elucidate the associations between olfactory structures and olfactory function.

3. Assess the effects of MetS and insulin resistance, as measured by fasting serum insulin (FSI) and HOMA-IR, on brain structures.

I based my work on data from the first 2000 participants enrolled in the Rhineland Study. To be able to address the questions regarding involvement of olfactory brain structures, I first had to develop the tools to measure these. In **Chapter 2** I describe the development of a reliable manual segmentation protocol of the olfactory bulb, which was implemented in the Rhineland Study. In **Chapter 3,** I describe the association of MetS and insulin resistance with olfactory structures and function. In **Chapter 4**, I firstly examined how olfactory structures assessed by MRI relate to olfactory function, and then determined to what extent OBV mediates the association between central olfactory structures and olfactory dysfunction across the lifespan. In **Chapter 5**, I assessed the association of MetS and insulin resistance with brain morphology, as well as the role of insulin resistance in the MetS-related brain alteration.

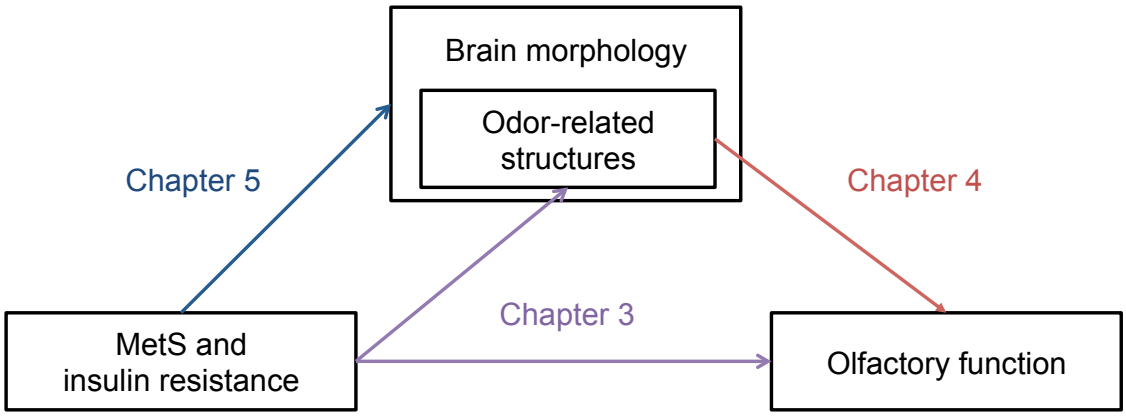

Figure 1.1 Illustration of the aims of the thesis

2. Segmentation of the olfactory bulb

INTRODUCTION

The olfactory bulb, as the first relay in the odor pathway, plays an important role in integrating peripheral and central processing of odor information. It processes afferent olfactory information from olfactory receptor neurons and passes it to the primary olfactory cortex.[106]

In both animal and human studies, smaller olfactory bulb volume (OBV) has been associated with a decreased number of cells.[107,108] Hence, it has been suggested that OBV could potentially be an indicator of olfactory function. In 1989, Suzuki and his colleagues for the first time described the observation of the olfactory bulb and tract in human MRI.[109] From then on, a few studies have reported an association between OBV as assessed by MRI and olfactory function in both patients with various pathological conditions, as well as in small series of healthy subjects.[31,33,110-112] Thus far, the relation between OBV and olfactory function has not been evaluated in the general population.

Currently, automated segmentation of the olfactory bulb is not available. Until now, only manual segmentations have been performed in small-scale studies and mainly based on anisotropic MRI scans acquired on 1.5 Tesla scanners. Since the olfactory bulb is a tiny structure in the forebrain, the resolution of the images could potentially have a large influence on the accuracy of the segmentation. We aimed to develop, validate and implement a reliable protocol for manual segmentation of the olfactory bulb in the high-resolution images that we are requiring in the Rhineland Study. These manual annotations will provide the basis for the further development of an automated segmentation algorithm.

METHODS

Subjects

The current work was based on the first 639 participants (enrolled between March 2016 and October 2017) who underwent brain imaging in the Rhineland Study. Among them, 82 participants were excluded due to insufficient imaging quality (n=67), lack of T2-weighted sequence (n=5), lack of MRI-derived measures from the T1-weighted images (n=10). Therefore, manual segmentation of left and right OBV was performed on 557 participants.

Manual annotation

Blinded to all other participant information, i.e. outcomes of the olfactory testing and demographic information, the manual segmentation of the left and right olfactory bulb was performed on T2-weighted images (details described in **Chapter 1.4**) using a multi-view approach (axial, coronal and sagittal) with Freeview, a visualization tool of FreeSurfer version 6.0. The images were not modified with any pre-processing step before manual annotation. A fixed window/level of 850/350 was assigned before labeling.

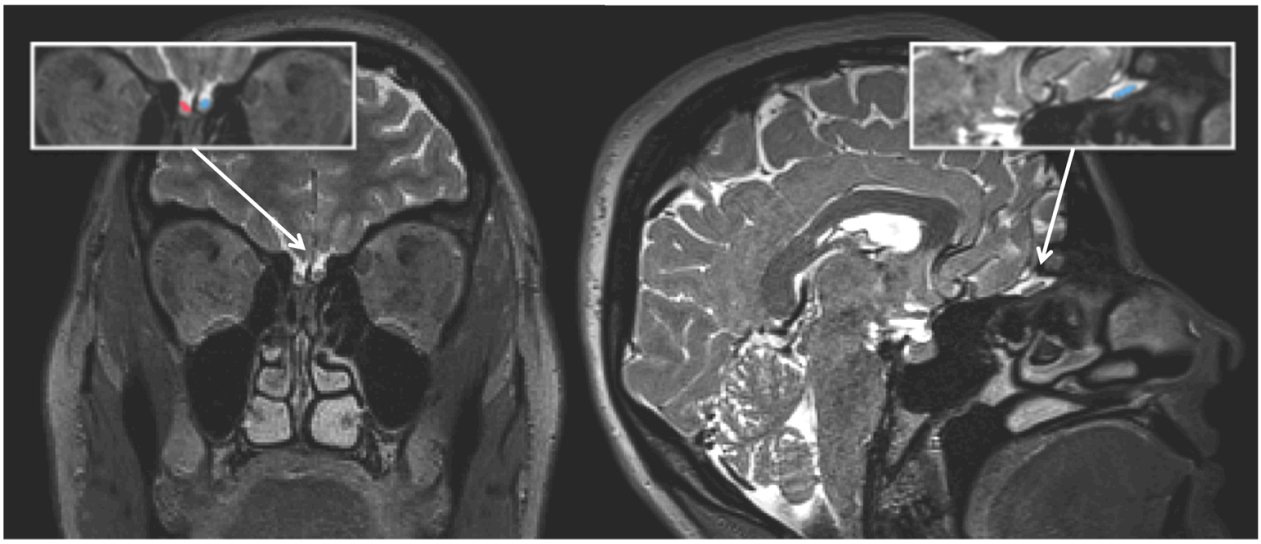

Figure 2.1 Coronal and sagittal depictions of the annotated olfactory bulb volumes (OBVs) on T2-weighted images

The left and right OBV are labeled in blue and red, respectively.

The olfactory bulb is a mostly almond- or spindle-shaped structure symmetrically located at the base of the forebrain (**Figure 2.1**). The boundaries of the olfactory bulb were mainly demarcated based on surrounding cerebrospinal fluid and the underlying cribriform plate. The abrupt change in diameter at the beginning of the olfactory tract in axial and sagittal views was used as the marker of the posterior end.[113,114]

Using a voxel-wise approach, all slices through the olfactory bulb were labeled manually by an experienced rater (R.L.). Different labels were used for the left and right olfactory bulb, respectively. OBVs in cubic millimeters (mm^3) were calculated by summing up the total number of labeled voxels and multiplying by voxel size. In cases where the olfactory bulb was not visible on MRI, OBV was defined as zero. To additionally assess intra- and inter-rater reliability, 50 scans were randomly chosen for repeated measurements by the same rater as well as another experienced rater.

Automated segmentation

An automated segmentation method is being developed based on the aforementioned manual annotations using supervised deep learning approaches. Different 2D and 3D deep learning models are being implemented on T1- and T2-weighted images.

Statistical analysis

The intra- and inter-rater reliability was evaluated by calculating the intraclass correlation coefficient (ICC), using a two-way design and based on absolute agreement. In addition, we used the Dice similarity coefficient (DSC) to assess the absolute agreement between measures in terms of volume and spatial position.[115] When both A (repeated measure) and B (initial measure) denote a binary segmentation, the Dice score is defined as: $DSC = 2 |A \cap B| / (|A|+|B|)$, where $|A|$ and $|B|$ are the number of elements in each segmentation, and $|A \cap B|$ is the number of shared elements. Therefore, a higher DSC represents a better agreement between segmentations in a voxel-voxel manner.

Pearson correlation coefficient was computed between left and right OBVs. Multivariable linear regression was used to assess the effect of age and sex on bilateral OBV after adjustment for the Estimated Total Intracranial Volume (eTIV), an indicator of head size generated from the FreeSurfer pipeline.

RESULTS

The manual segmentation was performed in 557 participants (56.9% women) with a mean (standard deviation, SD) age of 53.7 (13.2) years.

There was good-to-excellent reliability of our manual segmentation method: ICC (95% confidence intervals [95% CI]) for the left and right OBV was 0.965 (0.960; 0.980) and 0.985 (0.970; 0.992) for intra-rater reliability, and 0.845 (0.703; 0.916) and 0.880 (0.799; 0.930) for inter-rater reliability. The variability as assessed by DSC showed a similar result: for the left and right OBV intra-rater DSC expressed as mean (SD) was 0.934 (0.052) and 0.940 (0.043), and inter-rater DSC 0.816 (0.068) and 0.824 (0.077).

The OBVs varied over a wide range among participants (left: from 0 [i.e. aplasia] to 55.30 mm^3; right: from 0 to 55.81 mm^3), but were relatively consistent within participants (correlation coefficients [95% CI] between left and right OBVs: 0.867 [0.844 to 0.886]). Using multivariable linear regression, we observed that both left and right OBV were larger in men and decreased with increasing age after adjustment for head size (Difference [95%CI] in OBV (mm^3) was -0.15 [-0.20, -0.10] per 1-year increase of age and 2.35 [0.66, 4.05] in men compared to women for the left side, and -0.15 [-0.20, -0.09] per 1-year increase of age and 2.59 [0.76, 4.42] in men compared to women for the right side).

An automated segmentation method is under development currently. The DSC of our current preliminary deep-learning method was similar to inter-rater variability.

DISCUSSION

In this study, we presented a reliable manual segmentation method of the olfactory bulb for high-resolution (0.8×0.8×0.8 mm^3) T2-weighted images. The method showed good-to-excellent intra- and inter-rater reliability. The DSC of the preliminary deep-learning based automated segmentation was comparable to the inter-rater performance.

Our manual segmentation protocol was implemented in a large sample of individuals from a population-based study with a wide range of age (30 - 87 years). In addition, the

segmented OBV presented similar characteristics that were reported in another study in healthy subjects:[31] OBVs of both left and right side were larger in men and were inversely associated with age. Therefore, we consider our manual segmentations provide robust data to be used in subsequent analyses (**Chapter 3** and **4**). Moreover, they provide relevant input data for the further development of automated segmentation of the olfactory bulb.

Although manual segmentation is always considered as gold standard for volumetric measures assessed by MRI, it is a time-consuming process and relies on the experience of the rater. Thus, automated segmentation is required, especially for large population-based longitudinal studies. Our current work on the development of automated method for olfactory bulb segmentation showed promising initial results. However, achieving good accuracy of OBV is still challenging due to the location, small-size volume, inhomogeneous intensity,[116] and interference of neighboring vessels. The development of a fully automated segmentation method is therefore beyond the scope of the current thesis.

3. Metabolic syndrome and insulin resistance in relation to olfactory structure and function

INTRODUCTION

Olfactory dysfunction, i.e. a diminished ability to identify odors, is a highly prevalent but relatively understudied condition, which is especially common in the elderly and has been associated with several neurodegenerative as well as metabolic disorders.[2] Olfactory dysfunction has been related to various components of the metabolic syndrome (MetS), including obesity, diabetes mellitus and hypertension.[3,4] Recent studies also found a higher prevalence of self-reported olfactory dysfunction in subjects with MetS.[9,10] Despite the high prevalence of olfactory dysfunction, less than a quarter of individuals with smell dysfunction are cognizant of their sensory impairment until formally tested.[11] It is still unknown whether, and to what extent, objectively quantified olfactory function is associated with either MetS or insulin resistance, its core pathogenic element, in the general population.

Although a higher prevalence of olfactory dysfunction or a poorer olfactory function was observed in the presence of MetS and its individual components, the underlying mechanism remains elusive. Peripheral insulin, as the main source of insulin in the brain, crosses the blood-brain barrier via brain insulin receptors, which are densely packed in olfactory brain regions.[83-85] This spatial overlap, therefore, suggested a link between insulin and olfaction. Subsequent studies found that central insulin signaling decreased odorant-induced electro-physiological activity in olfactory sensory neurons and modulated the ion channels in the olfactory bulb in rodents,[5,7,88] while attenuated smell capacity after short-term hyperinsulineamia was observed in healthy subjects.[89,90] It is well known that insulin resistance plays a pivotal role in the pathogenesis of MetS.[23] Therefore, we hypothesized that MetS, and in particular insulin resistance, could lead to olfactory dysfunction, possibly through an effect on olfaction-related brain structures.

To assess our hypothesis, we aimed to investigate in a population-based cohort the association of MetS and insulin resistance with olfaction, both structurally and functionally.

RESEARCH DESIGN AND METHODS

Study design

The Rhineland Study is an ongoing population-based prospective cohort initiated in 2016 in residents aged 30 years and above in Bonn, Germany.[99] Approval to undertake the study was obtained from the ethics committee of the University of Bonn, Medical Faculty. The study was carried out in accordance with the recommendations of the International Conference on Harmonisation (ICH) Good Clinical Practice (GCP) standards (ICH-GCP). Written informed consent was obtained from all participants in accordance with the Declaration of Helsinki.

Assessment of metabolic syndrome

Waist circumference was measured with a flexible anthropometric tape (SECA 201) to the nearest millimeter at the midpoint between the last rib and iliac crest. Blood pressure was measured three times over half an hour with an oscillometric blood pressure device (OMRON 705 IT) in a semi-recumbent position, and the second and the third measures were averaged. Blood samples were collected after an at least 8-hour fast. Fasting serum insulin (FSI), triglycerides and HDL-C were measured using standard protocol in the central lab of University Hospital of Bonn. Fasting plasma glucose (FPG) concentration was measured on the Nightingale platform (Nightingale Health, Helsinki, Finland).[103] Homeostatic assessment of insulin resistance (HOMA-IR) was calculated on the basis of fasting values of glucose and insulin as HOMA-IR = fasting glucose in mmol/L × fasting insulin in mIU/L / 22.5.[104] Participants provided information regarding any anti-diabetic, anti-hypertensive and lipid-modifying medications used currently and in the past 12 months.

The presence of MetS was defined in accord with the revised National Cholesterol Education Program Adult Treatment Panel III (NCEP - ATP III) criteria[117,118], i.e. 1) waist circumference ≥ 102 cm in men and ≥ 88 cm in women, 2) triglyceride ≥ 150 mg/dl or treatment for hypertriglyceridemia, 3) HDL-C < 40 mg/dl in men and < 50 mg/dl in women or treatment for reduced HDL-C, 4) systolic and diastolic blood pressure (BP) ≥ 130/85 mmHg or on antihypertensive drug treatment, and 5) fasting plasma glucose

(FPG) ≥ 100 mg/dl or on drug treatment for elevated glucose. Participants were diagnosed as having MetS if they fulfilled at least 3 of the 5 criteria.

Assessment of olfactory function

Olfactory function was assessed by 12-item "Sniffin' Sticks" odor identification test (SIT-12).[105] Participants were presented each of twelve felt-tip sticks from the test kit (Burghart Messtechnik GmbH, Germany) approximately 2 cm from their nose for 3 to 4 seconds with an at least 20-second interval, and they had to choose one of the four answer options for each odorant. The sum of the correct responses was calculated as the final score (range: 0-12). Self-reported nasal patency was recorded as "blocked" or "free" and was used as an indicator of general nasal condition.

MRI acquisition

MRI scans were obtained on 3T Siemens MAGNETOM Prisma MRI scanners (Siemens Healthcare, Erlangen, Germany) equipped with 64-channel head-neck coils in two examination sites in Bonn, Germany. A three-dimensional T1-weighted magnetization-prepared rapid gradient-echo (MPRAGE) sequence (acquisition time = 6.5 min, repetition time = 2560 ms, inversion time = 1100 ms, flip angle 7°, field of view = 256×256 mm, voxel size = 0.8×0.8×0.8 mm^3),[100,101] and a T2-weighted sequence using a sampling perfection with application-optimized contrasts by using flip angle evolution (SPACE, repetition time = 2800ms, echo time = 405ms, field of view = 256×256 mm, voxel size = 0.8×0.8×0.8 mm^3) were acquired.

Image Processing

All T1-weighted images were processed using FreeSurfer version 6.0 (http://surfer.nmr.mgh.harvard.edu/). Seven regions of interest were selected based on their known involvement in the olfactory pathway:[24] entorhinal cortex, amygdala, parahippocampal cortex, hippocampus, insular cortex, as well as lateral and medial orbitofrontal cortex. Manual annotation of bilateral olfactory bulb on T2-weighted images was performed with Freeview by an experienced rater (R.L.), who was blinded to all other participant's information, i.e. outcomes of the olfactory testing and demographic information. The delineation of the OBV was mainly determined by the surrounding

cerebrospinal fluid and the underlying cribriform plate. The abrupt change in diameter of the olfactory bulb was used as the marker of the posterior end.[113,114] The volume (mm^3) of the olfactory bulb was calculated based on the total number of labeled voxels. In cases where the olfactory bulb was absent or could not be detected on the MRI scans, OBV was defined as zero. Fifty scans were randomly selected for repeated measurements by the same rater as well as another experienced rater to assess intra- and inter-rater reliability, respectively. Volumetric measures from the right and left hemisphere were averaged. The Estimated Total Intracranial Volume (eTIV) generated by FreeSurfer was used as an indicator of head size. Intra-rater and inter-rater reliability analyses revealed good to excellent agreement: the intra-class coefficient was 0.976 (95% confidence intervals [95% CI], 0.962 to 0.984) for intra-rater reliability, and 0.862 (95% CI, 0.802 to 0.905) for the inter-rater reliability, respectively.

Study population

The current investigation was based on the first 2000 participants (enrolled between March 2016 and June 2018) of the Rhineland Study. Of these, a subsample of 1158 participants had brain structural MRI scans. Among them, information for SIT-12, FSI, HOMA-IR and MetS was available for 1117, 1059, 1019, 995 individuals, respectively. Therefore, a total of 960 participants had a complete data on SIT-12, MetS, insulin resistance, MetS and brain MRI. An additional 20 participants were excluded due to the presence of cerebral infarction or bleeding (n=12), intracranial tumor (n=5) or other parenchymal congenital or acquired defects (n=3) on brain imaging, leaving 940 participants available for analysis. The participants included in the analyses were younger, had lower level of insulin resistance, and better metabolic status than those without complete data (**Table 3.1**).

Blinded to the outcomes of the odor identification test and demographic information, in the first 639 participants who had undergone brain imaging (enrolled between March 2016 and October 2017), bilateral olfactory bulb volumes (OBVs) were manually segmented on T2-weighted images. Eighty-two participants were excluded due to poor image quality (n=67), lack of T2-weighted scans (n=5) or lack of MRI-derived measures form T1-weighted images (n = 10). Therefore, OBVs could eventually be estimated in

557 participants. An additional 130 participants were excluded because of lack of information on insulin resistance, individual components of MetS and SIT-12 score, leaving 427 participants for a subsample analysis of the relation between insulin resistance, MetS and OBV.

Table 3.1 Characteristics of the participants included and excluded in the study

Characteristic[1,2]	Included	Excluded	Adjusted P value[3]
N	940	1060	
Age, year	52.3 (13.5)	57.2 (14.3)	<0.001
Women, n (%)	530 (56.4)	604 (57.0)	0.823
SIT-12	9.9 (1.5)	9.7 (1.9)	0.697
Nasal patency as "blocked", n (%)	164 (17.4)	221 (20.8)	0.105
Waist circumference, cm	86.7 (12.4)	89.6 (14.5)	<0.001
Triglyceride, mg/dL	111.4 (71.9)	115.9 (74.9)	0.357
HDL-C, mg/dL	65.6 (18.7)	63.1 (18.4)	<0.001
Systolic BP, mmHg	127.7 (15.8)	128.5 (17.1)	0.009
Diastolic BP mmHg	77.3 (9.4)	76.6 (9.8)	0.014
FPG, mmol/L	4.0 (0.5)	4.2 (0.9)	<0.001
FSI, mIU/L	9.6 (6.1)	10.7 (7.8)	0.007
HOMA-IR, unit	1.8 (1.3)	2.1 (1.9)	0.001

Abbreviations: SIT-12, 12-item "Sniffin' Sticks" odor identification test; HDL-C, High-density lipoprotein cholesterol; BP, blood pressure; FPG, fasting plasma glucose; FSI, fasting serum insulin; HOMA-IR, homeostatic assessment of insulin resistance.
[1] The characteristic of the participants was expressed as mean (SD) or count (percentage).
[2] Missing data in participants included and excluded in the study: SIT-12: 0 *vs*. 85; nasal patency: 0 *vs.* 4; waist circumference: 0 *vs.* 13; triglyceride and HDL-C: 0 *vs.* 195; BP: 8 *vs.* 23; FPG: 0 *vs.* 108; FSI: 0 *vs.* 202; HOMA-IR: 0 *vs.* 270.
[3] Age- and sex-adjusted

Statistical analyses

Age- and sex- adjusted intergroup differences were compared using multivariable linear regression for continuous variables, and logistic regression for categorical variables, respectively. Separate multivariable linear regression models were used: *1)* to assess the association between MetS and insulin resistance and olfactory brain structures adjusted for age, sex and head size, and *2)* to determine the association between MetS and insulin resistance and olfactory function adjusted for age, sex, and nasal patency.

Continuous and categorical variables are reported as means and standard deviations (SD) or counts and percentages, respectively. Statistical significance was defined as a two-tailed $P < 0.05$. All statistical analyses were performed in R version 3.4.[119]

RESULTS

Demographics of the study population

Of the 940 participants, 100 (10.6%) met three or more revised NCEP - ATP III criteria, and thereby fulfilled the requirements for a formal MetS diagnosis. Compared to those without MetS, participants with MetS were older (mean difference [95% CI] = 6.5 [4.0, 9.1] years), more often men (57.5% *vs.* 47.0%, P = 0.058) and had higher levels of insulin resistance (age- and sex-adjusted difference [95% CI]: 7.9 [6.7, 9.1] mIU/L for FSI, and 1.8 [1.5, 2.0] for HOMA-IR). By definition, they scored worse on all the separate MetS components (age-adjusted difference [95% CI]: 16.6 [14.6, 18.5] cm for waist circumference, 104.7 [91.7, 117.7] mg/dL for triglyceride levels, -19.5 [-22.7, -16.3] mg/dL for HDL-C levels, 9.7 [6.9, 12.6] and 5.8 [3.9, 7.7] mmHg for systolic and diastolic blood pressure, and 0.5 [0.4, 0.6] mmol/L for FPG levels, **Table 3.2**).

Metabolic syndrome and olfactory structures

The age-, sex- and head size-adjusted associations between MetS, insulin resistance and volumes of olfactory brain structures are summarized in **Table 3.3**. Higher levels of FSI and HOMA-IR and the presence of MetS were associated with smaller volumes of odor-related brain structures, except for amygdala, parahippocampus and hippocampus. These associations were most outspoken, and reached statistical significance, for entorhinal cortex, insula, and lateral and medial orbitofrontal cortex.

Metabolic syndrome and olfactory function

Neither MetS nor insulin resistance was associated with olfactory function as measured by the SIT-12 (difference [95% CI] in SIT-12 score: 0.04 [-0.26, 0.34] in participants with MetS compared to those without, -0.04 [-0.14, 0.05] per 1-SD increase of FSI, -0.03 [-0.12, 0.06] per 1-SD increase of HOMA-IR) after accounting for age, sex and nasal

patency.

Table 3.2 Characteristics of the study population

Characteristic[1]	Overall	With MetS	Without MetS
N	940	100	840
Age, year	52.3 (13.5)	58.1(12.1)	51.6 (13.5)
Women, n (%)	530 (56.4)	47 (47.0)	483 (57.5)
SIT-12	9.9 (1.5)	9.7 (1.4)	10.0 (1.5)
Nasal patency as blocked, n (%)	164 (17.4)	24 (24.0)	140 (16.7)
Waist circumference, cm	86.7 (12.4)	103.5 (10.6)	84.7 (11.1)
Triglyceride, mg/dL	111.4 (71.9)	208.9 (110.3)	99.8 (55.5)
HDL-C, mg/dL	65.6 (18.7)	48.0 (11.7)	67.7 (18.3)
Systolic BP, mmHg[2]	127.7 (15.8)	139.8 (14.2)	126.3 (15.3)
Diastolic BP mmHg[2]	77.3 (9.4)	83.3 (9.7)	76.6 (9.1)
FPG, mmol/L	4.0 (0.5)	4.5 (0.9)	3.9 (0.4)
FSI, mIU/L	9.6 (6.1)	16.8 (8.9)	8.8 (5.1)
HOMA-IR, unit	1.8 (1.3)	3.4 (1.9)	1.6 (1.0)

Abbreviations: MetS, metabolic syndrome; SIT-12, 12-item “Sniffin’ Sticks” odor identification test; HDL-C, High-density lipoprotein cholesterol; BP, blood pressure; FPG, fasting plasma glucose; FSI, fasting serum insulin; HOMA-IR, homeostatic assessment of insulin resistance.

[1] The characteristic of the participants was expressed as mean (standard deviation) or count (percentage).

[2] There were eight participants (6 without MetS and 2 with MetS) without the measurement of systolic and diastolic BP.

Table 3.3 The association of MetS and insulin resistance with olfactory brain structures

	Standardized volume difference (95% CI) [1]							
	OBV [2]	EC	Amy	PHC	HC	IC	lOFC	mOFC
FSI (per SD)	-0.02 (-0.11, 0.07)	-0.06* (-0.13, -0.00)	0.03 (-0.02, 0.07)	-0.05 (-0.11, 0.01)	0.02 (-0.02, 0.07)	-0.05* (-0.10, -0.01)	-0.04 (-0.08, 0.01)	-0.05* (-0.10, -0.01)
HOMA-IR (per SD)	-0.02 (-0.12, 0.07)	-0.07* (-0.13, -0.01)	0.02 (-0.03, 0.07)	-0.04 (-0.10, 0.01)	0.02 (-0.02, 0.07)	-0.05* (-0.10, -0.01)	-0.04 (-0.08, 0.01)	-0.05* (-0.10, -0.01)
MetS: with *vs.* without	-0.22 (-0.53, 0.08)	-0.08 (-0.28, 0.11)	0.09 (-0.06, 0.24)	0.12 (-0.06, 0.31)	0.06 (-0.09, 0.20)	-0.16* (-0.30, -0.02)	-0.14* (-0.27, 0.00)	-0.23** (-0.37, -0.09)

Abbreviations: FSI, fasting serum insulin; HOMA-IR, homeostatic assessment of insulin resistance; MetS, metabolic syndrome; OBV, olfactory bulb volume; EC, entorhinal cortex; Amy, Amygdala; PHC, parahippocampal cortex; HC, hippocampus; IC, insular cortex; lOFC, lateral orbitofrontal cortex; mOFC, medial orbitofrontal cortex.

[1] Volumetric measures from the right and left hemisphere were averaged and standardized.

[2] The relation between insulin resistance and MetS and OBV was evaluated in a subsample of 427 participants.

* P<0.05; ** P<0.01

DISCUSSION

In this cross-sectional analysis of a population-based cohort, we found that MetS and insulin resistance were associated with several olfactory structures, i.e. entorhinal, insula, and lateral and medial orbitofrontal cortex, but not with the performance on a quantitative olfactory function test.

The present study provides a comprehensive examination of the relation between MetS and insulin resistance and odor-related brain structures, starting from the olfactory bulb, the first relay of the odor pathway, all the way up to the distal orbitofrontal cortex. We found that several odor-related brain regions, including the entorhinal cortex, insula, and lateral and medial orbitofrontal cortex, were smaller in subjects with higher insulin resistance or MetS. Our findings are in line and extend previous reports describing associations between the volumes of the insula and particularly the orbitofrontal cortex, as a part of the prefrontal cortex, and some of the constituting components of MetS, including obesity, type 2 diabetes mellitus and hypertension, as well as insulin resistance.[44,50,54,58,59,73] The association of MetS and insulin resistance with OBV has not been assessed before. We found a pronounced, albeit - presumably because of a relative small sample size - not statistically significant negative effect of MetS on the volume of olfactory bulb.

In contrast to reports of a higher prevalence of self-reported olfactory dysfunction in individuals with MetS in Korean populations,[9,10] using objective measures of olfactory function instead of self-reports, we failed to find an association between MetS, insulin resistance and odor identification function. Since no other studies are available so far in the European population, we cannot rule out potential population-specific effects. However, the discrepancy between subjective and objective olfactory dysfunction measures has been well-documented in previous epidemiological studies,[2,120] with a generally poor correlation of self-reported olfactory function with results on objective tests.[121] Therefore, lack of objective, quantitative measures of olfactory function may underlie previous reports of an association between MetS and olfactory dysfunction.[9,10]

In the current study, MetS and insulin resistance had different associations with olfactory structures and functions. Thus, question arises as to how olfactory structures are related

to olfactory function. No study so far has examined this structural-functional relationship in olfaction systematically. Several studies suggested that some odor-related structures, especially OBV and volume of orbitofrontal cortex, was associated with olfactory function in patients,[26-29,111,122] as well as in the healthy individuals.[31-33] However, these small-scale studies were mainly enrolled young subjects in a clinical setting. Only recently, a cohort study showed that impaired olfactory function was related to smaller volumes of hippocampus and entorhinal cortex in dementia-free elderly.[16] Therefore, future studies should further examine whether and to what extent olfactory brain structures are associated with olfactory function in the general population across the lifespan.

Strengths of the study include large sample size drawn from a population-based cohort, a wide range of age, high-resolution MRI scans, and comprehensive data on both olfactory structures and function. However, the present study also has certain limitations. First of all, the cross-sectional design limited our inference of causality. In addition, we used solely odor identification, a subtask of the olfactory testing battery. Compared to other psychophysical tests, the identification test is widely used due to its practicality,[123] and the results from the majority of such tests were shown to be correlated with one another.[124] However, it is still of interest to have further studies to evaluate olfaction in MetS and insulin resistance using a more complete olfactory psychophysical test covering other features, i.e. threshold and discrimination. Moreover, the prevalence of the MetS is low (i.e. 10.6%) in our study compared to other studies in the Europe.[125-127] Therefore, the replication of our findings in other population-based studies is needed.

In conclusion, in a population-based cohort, we found that MetS and insulin resistance were associated with several olfactory brain structures, but not with olfactory function. As the first population-based study to evaluate both olfactory function and its neuroanatomical correlates in MetS and insulin resistance, our findings shed new light on the metabolic influence on the olfaction. More evidence from future epidemiological studies is warranted to better understand the effects of MetS and insulin resistance on olfaction.

4. Disentangling the structural components of olfactory dysfunction in the general population

INTRODUCTION

Olfactory dysfunction, defined as an absent or reduced sense of smell, could affect up to one-fourth of the adult general population.[2] It has been associated with age, male sex, smoking, head trauma and chronic rhinosinusitis,[128] although little is known about its determinants in relatively young individuals, i.e. those aged less than 50 years. Importantly, impaired olfactory function is among the earliest signs of many neurodegenerative disorders, including Alzheimer's disease and Parkinson's disease, and often precedes formal diagnosis by many years.[11,13,129] It is therefore of importance to elucidate its neuroanatomical basis as this could provide insights into its underlying causes, and in addition, facilitate identification of individuals at an increased risk of developing neurodegenerative conditions later in life.

Olfactory function has been evaluated through various psychophysical tests in both clinical and research settings, yet structural changes of the olfactory system have received little study. With the advent of high-field magnetic resonance imaging (MRI), it is now possible to obtain an objective and reliable assessment of the neuroanatomical correlates of olfactory function in large groups of individuals. The olfactory bulb, as the first relay in the olfactory pathway, plays an important role in the integration of peripheral and central processing of odor information. Following odor deprivation, olfactory bulb volume (OBV) was shown to decrease substantially, accompanied by marked changes in central projections to the olfactory bulb.[107,130] Moreover, previous small-scale studies found an association between OBV and olfactory dysfunction as assessed by psychophysical testing in both healthy subjects and patients with various neurological conditions.[33,131] However, this presumed relation between structure and function has not been consistently found in clinical cohorts,[132] nor has it been evaluated in the general population.

Recently, impaired odor identification was shown to predict cognitive decline and was associated with smaller volumes of the hippocampus as well as several other mesial temporal lobe structures.[16] However, it is still unknown whether this relation primarily reflects impaired central sensorineural processing, peripheral olfactory bulb pathology, or yet a combination of both. Given the appearance of neuropathological markers – including neurofibrillary tangles and alpha-synuclein aggregates – in the olfactory region prior to many other regions, it has been hypothesized that environmental insults might trigger olfactory bulb damage which then could spread to connected brain regions in a prion-like manner.[18] This hypothesis implies that pathology of olfactory epithelium and bulb would be the primary mediators of olfactory dysfunction. Alternatively, pathology of more downstream central olfactory structures may impair correct processing and identification of sensory information, especially in Alzheimer's disease.[18]

In order to gain a better understanding of the neuroanatomical basis of impaired olfaction, and disentangle the contribution of the different components of the olfactory pathway structures to its etiology, in the current study we aimed to assess 1) whether, and to what extent, structural alterations in the olfactory system are related to age-associated changes in olfactory function, and 2) to what extent OBV mediates the association between central olfactory structures and olfactory dysfunction across lifespan.

RESEARCH DESIGN AND METHODS

Study Design

We performed our analysis using baseline data from participants of the Rhineland Study, an ongoing population-based cohort study initiated in 2016. The study enrolls participants aged 30 years and above at baseline from Bonn, Germany.[99] Each participant undergoes a comprehensive 7-hour protocol including detailed brain imaging. Approval to undertake the study was obtained from the ethics committee of the University of Bonn, Medical Faculty. The study is carried out in accordance with the recommendations of the International Conference on Harmonization Good Clinical

Practice standards. We obtained written informed consent from all participants in accordance with the Declaration of Helsinki.

Image Acquisition

MRI scans were collected on two 3T Siemens MAGNETOM Prisma MRI scanners (Siemens Healthcare, Erlangen, Germany) equipped with 64-channel head-neck coils in two examination sites in Bonn. The standardized protocol included a T1-weighted multi-echo magnetization-prepared rapid gradient-echo (MPRAGE) sequence[101] with 2D acceleration[100] (acquisition time = 6.5 min, 4 echoes, repetition time = 2560 ms, inversion time = 1100 ms, flip angle = 7°, matrix size = 320×320×224, voxel size = 0.8×0.8×0.8 mm^3), and a bandwidth-matched T2-weighted 3D Turbo-Spin-Echo (TSE) sequence using variable flip angles[133] (SPACE, acquisition time = 5 min, repetition time = 2800ms, echo time = 405ms, turbo factor = 282, matrix size = 320×320×224, voxel size = 0.8×0.8×0.8 mm^3). Both sequences utilize elliptical sampling[100] for faster acquisition.

Image Processing

All T1-weighted images were processed using FreeSurfer version 6.0 (http://surfer.nmr.mgh.harvard.edu/) to derive quantitative volumetric measures. Based on their known role in the central processing of olfactory information, the entorhinal cortex, amygdala, parahippocampal cortex, hippocampus, insular cortex, and lateral and medial orbitofrontal cortex were selected as regions of interest for subsequent analysis.[24] We used the Estimated Total Intracranial Volume (eTIV) generated by FreeSurfer as proxy for head size.

Left and right OBVs were manually segmented on T2-weighted images using Freeview, a FreeSurfer visualization tool. The olfactory bulbs are mostly spindle-shaped structures symmetrically located at the base of the forebrain. The boundaries were demarcated based on surrounding cerebrospinal fluid and the underlying cribriform plate. The abrupt change in diameter of the olfactory bulb was used as the marker of the posterior end.[113,114] Using a voxel-wise approach, all slices through the olfactory bulb were labeled manually by an experienced radiologist (R.L.) who was blinded to all other

participant information. The labeled voxels were summed up to obtain the volume in cubic millimeters (mm^3). In cases where the olfactory bulb could not be detected on the MRI scan, OBV was defined as zero. Fifty scans were randomly chosen for repeated measurements by the same rater as well as another experienced rater to assess intra- and inter-rater reliability, respectively. The intra-class correlation coefficients showed good-to-excellent agreement: 0.976 (95% confidence intervals [95% CI], 0.962 to 0.984) for intra-rater reliability, and 0.862 (95% CI, 0.802 to 0.905) for inter-rater reliability, respectively.

Odor identification

The 12-item "Sniffin' Sticks" odor identification test (SIT-12) is a widely used screening test for assessing odor identification ability.[105] Each of the twelve felt-tip sticks from the test kit (Burghart Messtechnik GmbH, Germany) was positioned approximately 2 cm in front of both nostrils for 3 to 4 seconds. Participants were then asked to choose only one of the four answer options for each odorant. The time interval between two consecutive odor presentations was at least 20-seconds. The final score was generated as the total number of correct answers (range 0-12).

Questionnaire data

Smoking categories were defined as current, former and non-smoker. Nasal patency was reported as "blocked" or "free". All smoking and nasal patency information was based on self-reports.

Study Population

The present study is based on data from the first 2000 participants who were enrolled in the Rhineland Study between March 2016 and June 2018. Of these, 1915 had valid data on SIT-12. Blinded to the outcomes of the olfactory testing and demographic information, OBV was estimated based on bilateral manual segmentation of T2-weighted images in the first 639 participants (enrolled between March 2016 and October 2017) who had undergone brain imaging. In the end, 541 participants had complete data on all MRI-derived measures (including OBV) and SIT-12 and were used for subsequent analyses (**Figure 4.1**).

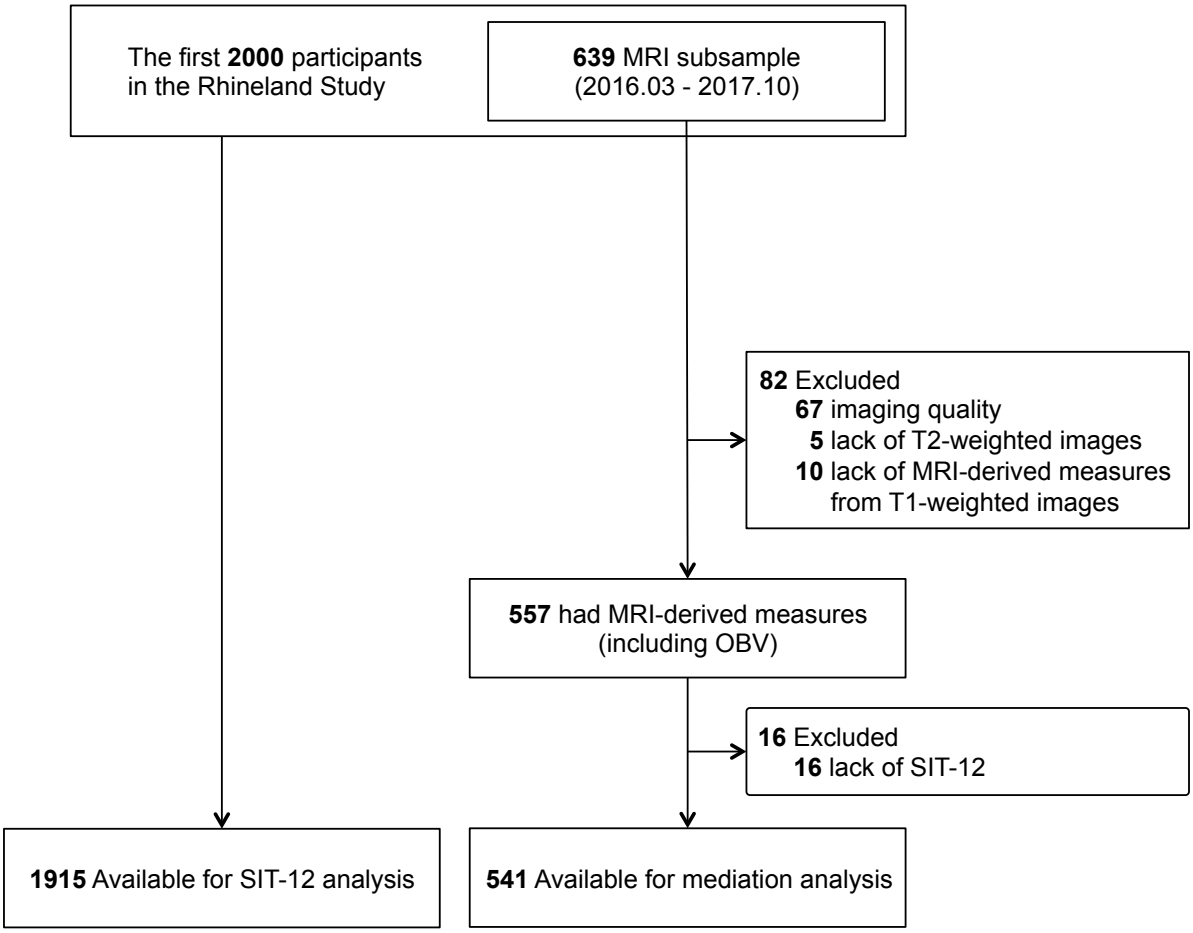

Figure 4.1 Selection of study participants in the Rhineland Study

Abbreviations: MRI, magnetic resonance imaging; SIT-12, 12-item "Sniffin' Sticks" odor identification test; OBV, olfactory bulb volume.

Statistical analyses

Descriptive data were expressed as mean (standard deviation, SD) or count (percentage) for continuous or categorical variables, respectively. Intergroup differences were compared with the Student's t-test for continuous variables and with the Pearson's chi-square test for categorical variables.

We used multivariable linear regression models to 1) examine the relation between previously reported determinants of odor identification function (age, sex, self-reported nasal patency and smoking) and SIT-12 score, 2) assess sex differences in OBV while accounting for age and head-size, 3) assess the associations between volumes of the

olfactory bulb and central olfactory structures with SIT-12 score while accounting for age, sex and nasal patency, and 4) assess associations between central olfactory structures and OBV. For the analyses performed under (3) and (4), the volumes of brain structures were averaged between left and right side, and head-size adjusted and normalized to the study population as follows: $Volume_{adjusted}$ = Volume / eTIV × $eTIV_{mean}$.

We subsequently assessed whether age modified any of the associations involving brain structures by testing for interaction effects between age and volumetric brain measures. In order to visualize the age-moderated association between olfactory structures and SIT-12, we plotted different regression lines for each tertile of age (i.e. 30-47, 47-59 and 59-87 years). Variance inflation factors were calculated to assess potential multi-collinearity among independent variables within the model. All model fits were corroborated by visual inspection of the distributions of the residuals.

To assess to what extent the relation between central olfactory structures and olfactory function was mediated through the olfactory bulb, we used structural equation modeling (**Figure 4.2**).[134] First, we performed a classical mediation analysis by constructing models with the volume of each central olfactory structure as the independent variable, the OBV as the mediator and the SIT-12 as the outcome variable (**Figure 4.2A**), while adjusting for age, sex and nasal patency. Second, because we found that age moderated the relations between volumes of brain olfactory structures and SIT-12 score in the multivariable regression analyses, we performed a moderated mediation analysis[135] by including age as a moderator to the paths directing from central olfactory structures and OBV to the SIT-12 score (**Figure 4.2B**), while additionally adjusting for sex and nasal patency. The 95% CIs of all the (moderated) mediation analysis estimates are based on non-parametric bias-corrected accelerated bootstrapping with 1000 re-samplings.

We performed multiple sensitivity analyses to evaluate the robustness of our findings. First, we repeated the analyses after exclusion of participants with aplasia of the olfactory bulb. Second, instead of using the average of the bilaterally measured OBV, we used the left and right OBV separately as the variable of interest. Statistical

significance was inferred at a two-tailed P < .05. All statistical analyses were performed in R version 3.4,[119] using the 'lavaan' package for structural equation modeling.[136]

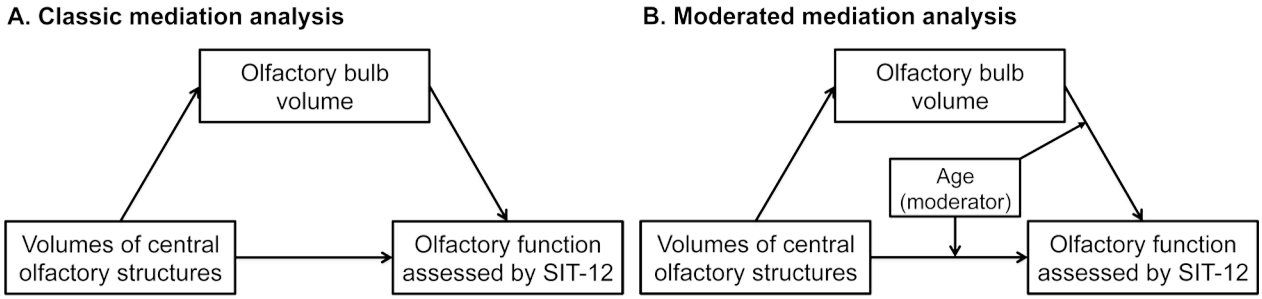

Figure 4.2 The mediation models

Abbreviation: SIT-12, 12-item "Sniffin' Sticks" odor identification test

RESULTS

Participant characteristics and olfactory function

Characteristics of the 1915 participants included in the analyses are shown in **Table 4.1**. The mean (SD) age was 54.5 (14.0; range: 30-95) years and 1084 (56.6%) were women. Overall, women had higher SIT-12 scores compared to men (9.9 (1.6) *vs.* 9.7 (1.8); P = .007), and reported less frequently nasal congestion (14.9% *vs.* 18.5%; P = .04). Individuals with MRI-derived measures available were on average slightly younger than those without brain imaging (53.6 (13.1) *vs.* 54.9 (14.4) years; P= .05) (**Table 4.1**). There were no differences in sex, SIT-12 score, self-reported nasal patency or smoking status between the two groups (**Table 4.1**).

The mean (SD) SIT-12 score of the participants in the Rhineland study was 9.8 (1.7). Ninety-four (4.9%) of them scored six or lower, indicating a high probability of having severe olfactory dysfunction.[105] Compared to the participants who scored ≥ 7, they were significantly older (69.7 (11.4) *vs.* 53.7 (13.7) years; P < .001) and more likely to be men (55.3% *vs.* 42.8%; P = .02). In general, olfactory function decreased with increasing age and was worse in men and in those who reported nasal congestion, both in the entire study sample as well as in the subgroup of participants with MRI-derived measures. We found no association between smoking and SIT-12 score (**Table 4.2**). Therefore, smoking was not included as a covariate in subsequent analyses.

Table 4.1 Characteristics of the study population

Characteristic	All participants	With MRI measures	Without MRI measures	P Value[1]
N	1915	541	1374	
Age, mean (SD), year	54.5 (14.0)	53.6 (13.1)	54.9 (14.4)	.05
Women, No. (%)	1084 (56.6)	306 (56.6)	778 (56.6)	>.99
SIT-12 score, mean (SD)	9.8 (1.7)	9.8 (1.7)	9.8 (1.7)	.85
Nasal patency as "blocked", No. (%)	315 (16.4)	88 (16.3)	227 (16.5)	.95
Smoking status, No. (%)[2]				.33
Current smoker	818 (47.4)	228 (50.2)	590 (46.5)	
Former smoker	678 (39.3)	166 (36.6)	512 (40.3)	
Non-smoker	228 (13.2)	61 (13.2)	167 (13.2)	

Abbreviations: SIT-12, 12-item "Sniffin' Sticks" odor identification test; MRI, magnetic resonance imaging

[1] Group differences between participants with and without MRI-derived measures were assessed with Student's t-test for continuous variables, and with Pearson's chi-square test for categorical variables.

[2] Missing data on smoking status: 177 overall, of whom 87 and 104 in participants with and without MRI-derived measures (including OBV), respectively.

Olfactory bulb volume

The OBVs varied over a wide range among participants (left: from 0 [i.e. aplasia] to 55.30 mm^3, right: from 0 to 55.81 mm^3), but left and right OBV were about equally sized within each individual (Pearson's correlation coefficient between left and right OBVs, 0.87; 95% CI, 0.84 to 0.89; P < .001). Men had larger OBVs than women on both left (age-adjusted difference, 3.97 mm^3; 95% CI, 2.62 to 5.31 mm^3; P < .001) and right sides (age-adjusted difference, 3.86 mm^3; 95% CI, 2.40 to 5.31 mm^3; P < .001). These differences became smaller but still statistically significant after accounting for head size (age- and head-size adjusted difference: left OBV 2.20 mm^3, 95% CI 0.47 to 3.92 mm^3, P = .01; right OBV: 2.55mm^3, 95% CI 0.68 to 4.42 mm^3, P = .008). On average, the OBV was larger on the right than on the left side (mean difference, 1.53 mm^3; 95% CI, 1.15 to 1.91 mm^3; paired t-test P < .001).

Table 4.2 The association of determinants with olfactory function using multivariable linear regression

	Difference (95% CI) in SIT-12 score			
	With SIT-12	With SIT-12 and smoking	With SIT-12 and MRI-derived measures	With SIT-12, MRI-derived measures and smoking
No. of participants	1915	1724	541	454
Age, year	-0.04** (-0.05, -0.04)	-0.04** (-0.05, -0.04)	-0.04** (-0.05, -0.03)	-0.04** (-0.06, -0.03)
Sex: men vs. women	-0.20** (-0.34, -0.05)	-0.17* (-0.32, -0.02)	-0.26 (-0.54, 0.02)	-0.24 (-0.55, 0.07)
Nasal patency: blocked vs. free	-0.21* (-0.41, -0.02)	-0.18 (-0.39, 0.02)	-0.28 (-0.66, 0.09)	-0.30 (-0.71, 0.12)
Smoking status:				
former vs. never	n/a	0.04 (-0.12, 0.20)	n/a	0.18 (-0.16, 0.51)
current vs. never	n/a	0.01 (-0.22, 0.24)	n/a	0.06 (-0.41, 0.53)

Abbreviations: SIT-12, 12-item “Sniffin’ Sticks” odor identification test; MRI, magnetic resonance imaging; OBV, olfactory bulb volume; n/a, not applicable.
* P < .05; ** P < .01

Relation between volumes of olfactory structures and olfactory function

After adjusting for age, sex and nasal patency, OBV was positively associated with olfactory function (difference in SIT-12 score, 0.51; 95%CI, 0.38 to 0.65; P < .01). No association was observed of other central olfactory structures with olfactory function (**Table 4.3**). However, as illustrated in **Figure 4.3**, we observed age-dependent associations between volumes of olfactory bulb, amygdala, parahippocampal cortex, and hippocampus and SIT-12 score, with each relationship being stronger in older subjects (P value for interaction between volume and age: 0.02, 0.05, 0.02, and 0.001, respectively; **Table 4.3**).

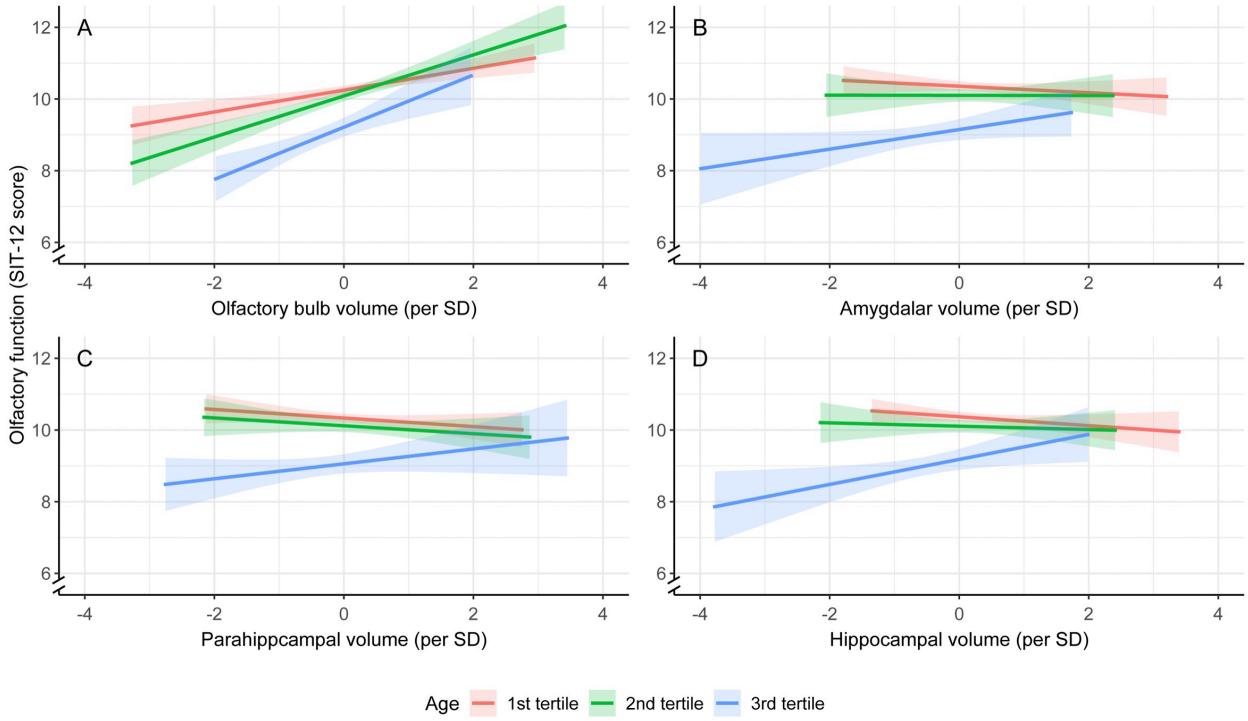

Figure 4.3 The relation between volumes of olfactory structures and olfactory function stratified by age

The associations between volumes of olfactory structures and olfactory function assessed by SIT-12 were modified by age. Lines represent the linear association between volumes of olfactory structures and SIT-12 score for each tertile of age (i.e. 30-47, 47-59 and 59-87 years), and the shadow area represents the 95% CIs. Volumetric measures from the right and left side were averaged, head-size adjusted, and normalized based on the overall 541 subjects.
Abbreviations: SIT-12, 12-item “Sniffin’ Sticks” odor identification test; OBV, olfactory bulb volume.

Table 4.3 Relation between volumes of olfactory brain structures and SIT-12 score

	Difference (95% CI) in SIT-12 score			
	Model 1	Model 2		
Olfactory brain structures[1,2]	volume	volume	age	volume × age
Olfactory bulb	0.51** (0.38, 0.65)	0.54** (0.41, 0.68)	-0.44** (-0.58, -0.30)	0.17* (0.03, 0.31)
Central olfactory structures				
Entorhinal cortex	-0.03 (-0.17, 0.11)	-0.03 (-0.17, 0.11)	-0.57** (-0.71, -0.43)	0.04 (-0.12, 0.19)
Amygdala	0.09 (-0.06, 0.24)	0.06 (-0.09, 0.21)	-0.52** (-0.67, -0.37)	0.16* (0.03, 0.29)
Parahippocampal cortex	-0.02 (-0.17, 0.12)	-0.04 (-0.18, 0.11)	-0.56** (-0.70, -0.41)	0.17* (0.03, 0.31)
Hippocampus	0.04 (-0.12, 0.19)	0.01 (-0.14, 0.16)	-0.51** (-0.67, -0.36)	0.22** (0.08, 0.35)
Insular cortex	-0.05 (-0.19, 0.09)	-0.05 (-0.19, 0.09)	-0.58** (-0.72, -0.44)	-0.01 (-0.14, 0.12)
Lateral orbitofrontal cortex	-0.04 (-0.18, 0.10)	-0.04 (-0.18, 0.10)	-0.58** (-0.72, -0.44)	0.02 (-0.12, 0.16)
Medial orbitofrontal cortex	0.03 (-0.11, 0.17)	0.04 (-0.10, 0.18)	-0.57** (-0.71, -0.43)	-0.08 (-0.21, 0.05)

Abbreviation: SIT-12, 12-item “Sniffin’ Sticks” odor identification test.
1 Volumetric measures from the right and left side were averaged, head-size adjusted, and normalized.
[2] Separate multivariable linear regressions were performed for each regional brain volumes with adjustment for age, sex, nasal patency
Model 1: SIT-12 ~ volume + age + sex + nasal patency
Model 2: SIT-12 ~ volume + age + sex + nasal patency + volume×age
* P< 0.05; ** P< 0.01

Relation between volumes of central olfactory structures and OBV

The volumes of the hippocampus and of the insular and medial orbitofrontal cortex were significantly associated with OBV after accounting for age, sex, and nasal patency (difference in OBV [per SD]: hippocampus, 0.11; 95% CI, 0.01 to 0.20; insular cortex, 0.12; 95% CI, 0.04 to 0.21; medial orbitofrontal cortex, 0.09; 95% CI, 0.01 to 0.17; **Table 4.4**). A similar trend was seen for the association between the amygdalar volume and OBV (difference in OBV [per SD], 0.08; 95% CI, -0.01 to 0.17; P = .08). These associations were not modified by age (**Table 4.4**).

Olfactory bulb as the mediator between central olfactory structures and olfactory function

Classical mediation analyses (**Figure 4.2A**) showed that the association between volumes of central olfactory structures (i.e. amygdala, hippocampus, insular cortex and medial orbitofrontal cortex) and odor identification (SIT-12 score) were mediated through OBV (**Table 4.2**). In addition, the moderated mediation analyses (**Figure 4.2B**) showed that the magnitude of the mediation through OBV was largely dependent on age: The indirect effect (i.e. the mediation effect through OBV) was consistently larger in older individuals. A statistically significant age-modified direct effect was only seen for the association between hippocampal volume and SIT-12 score, with the magnitude of the association sharply increasing with age (**Table 4.5**).

Sensitivity analyses

Similar results were obtained for left and right OBVs when analysed separately, and after exclusion of subjects with olfactory bulb aplasia (data not shown).

Table 4.4 Relation between volumes of central olfactory structures and olfactory bulb volume[1]

	Difference (95% CI) in OBV			
	Model 1	Model 2		
Central olfactory structures[2]	volume	volume	age	volume × age
Entorhinal cortex	0.00 (-0.08, 0.09)	0.00 (-0.08, 0.09)	-0.23** (-0.31, -0.14)	-0.03 (-0.13, 0.06)
Amygdala	0.08 (-0.01, 0.17)	0.08 (-0.01, 0.17)	-0.19** (-0.29, -0.10)	-0.02 (-0.10, 0.06)
Parahippocampal cortex	-0.06 (-0.15, 0.03)	-0.06 (-0.15, 0.03)	-0.23** (-0.31, -0.14)	0.03 (-0.05, 0.12)
Hippocampus	0.11* (0.01, 0.20)	0.12* (0.02, 0.21)	-0.20** (-0.29, -0.10)	-0.07 (-0.15, 0.01)
Insular cortex	0.12** (0.04, 0.21)	0.12** (0.04, 0.21)	-0.21** (-0.30, -0.13)	0.01 (-0.07, 0.08)
Lateral orbitofrontal cortex	0.02 (-0.06, 0.11)	0.03 (-0.06, 0.11)	-0.22** (-0.30, -0.14)	0.05 (-0.03, 0.13)
Medial orbitofrontal cortex	0.09* (0.01, 0.17)	0.10* (0.01, 0.18)	-0.22** (-0.30, -0.13)	-0.04 (-0.12, 0.04)

Abbreviations: OBV, olfactory bulb volume.
[1] Volumetric measures from the right and left side were averaged, head-size adjusted, and normalized.
[2] Separate multivariable linear regressions were performed for each regional brain volumes with adjustment for age, sex, nasal patency
Model 1: OBV ~ volume + age + sex + nasal patency
Model 2: OBV ~ volume + age + sex + nasal patency + volume×age
* P< 0.05; ** P< 0.01

Table 4.5 Mediation effect of OBV on the association of central olfactory structural volumes with olfactory function

Volume[1,2] of	Model [3,4]	Indirect effect	Direct effect	Total effect	Moderated mediation index[5]	OBV×Age[5]	Volume×Age[5]
Amygdala	Model A	0.039* (0.001, 0.087)	0.050 (-0.094, 0.213)	0.089 (-0.065, 0.269)			
	Model B	0.042* (0.001, 0.090)	0.017 (-0.121, 0.182)	0.059 (-0.095, 0.237)	0.011 (-0.002, 0.043)	0.144 (-0.045, 0.332)	0.151 (0.025, 0.298)
	1-SD below mean age	0.031* (0.003, 0.080)	-0.134 (-0.350, 0.045)	-0.103 (-0.324, 0.085)			
	1-SD above mean age	0.053* (0.001, 0.125)	0.168 (-0.030, 0.391)	0.221 (0.015, 0.445)			
Hippocampus	Model A	0.054* (0.014, 0.107)	-0.016 (-0.165, 0.138)	0.038 (-0.109, 0.201)			
	Model B	0.059* (0.015, 0.114)	-0.046 (-0.191, 0.099)	0.013 (-0.128, 0.166)	0.013 (-0.003, 0.045)	0.127 (-0.063, 0.307)	0.237 (0.105, 0.373)
	1-SD below mean age	0.045* (0.011, 0.099)	-0.284* (-0.473, -0.132)	-0.238* (-0.411, -0.067)			
	1-SD above mean age	0.072* (0.020, 0.151)	0.191 (-0.013, 0.430)	0.263* (0.045, 0.514)			
Insular cortex	Model A	0.065* (0.025, 0.124)	-0.113 (-0.264, 0.035)	-0.048 (-0.202, 0.096)			
	Model B	0.069* (0.020, 0.117)	-0.109 (-0.242, 0.024)	-0.040 (-0.180, 0.099)	0.021 (-0.001, 0.043)	0.169 (0.033, 0.306)	-0.027 (-0.150, 0.097)
	1-SD below mean age	0.048* (0.008, 0.088)	-0.082 (-0.273, 0.109)	-0.034 (-0.226, 0.158)			
	1-SD above mean age	0.090* (0.025, 0.154)	-0.136 (-0.307, 0.035)	-0.046 (-0.227, 0.134)			
Medial orbitofrontal cortex	Model A	0.047* (0.002, 0.109)	-0.018 (-0.196, 0.139)	0.029 (-0.150, 0.195)			
	Model B	0.050* (0.003, 0.113)	-0.004 (-0.171, 0.145)	0.046 (-0.128, 0.205)	0.016 (-0.001, 0.048)	0.170 (-0.021, 0.352)	-0.068 (-0.238, 0.100)
	1-SD below mean age	0.034* (0.003, 0.098)	0.064 (-0.133, 0.240)	0.098 (-0.112, 0.290)			
	1-SD above mean age	0.065* (0.005, 0.150)	-0.071 (-0.365, 0.174)	-0.006 (-0.300, 0.238)			

Abbreviations: OBV, olfactory bulb volume

[1] Separate mediation analyses were performed for each regional brain volumes.

[2] Volumetric measures from the right and left side were averaged, head-size adjusted, and normalized.

[3] Model A: without age as a moderator; Model B: with age as a moderator.

[4] The β (95% CI) of moderated mediation analysis was reported of mean age, and 1-SD below and above the mean age.

[5] The moderated mediation index and interaction effects were presented only for Model B

* Statistically significant (95% CIs did not contains 0)

DISCUSSION

In this large-scale population-based cohort of adults aged 30 years and above, we found a strong association between larger OBV and better odor identification function across all age groups, independent of other established determinants of olfactory function including sex, nasal patency and smoking. We also found an age-dependent association between the volumes of several key central olfactory brain structures (i.e. amygdala, parahippocampal cortex and hippocampus) and olfactory function that was predominantly present in older age groups. Importantly, we additionally identified OBV as a robust mediator of the association between the volumes of amygdala, hippocampus, insular and medial orbitofrontal cortex and odor function, where the mediation effect consistently increased with older age.

To the best of our knowledge, this is the first population-based study evaluating the interconnections between the olfactory bulb and central olfactory structures and odor identification function simultaneously. Our findings highlight the unique mediatory role of the olfactory bulb in the odor pathway: OBV was not only consistently associated with olfactory function and the core components of the central olfactory system across lifespan, but also largely mediated the association between the volumes of central olfactory structures and odor function. Unlike other subcortical and cortical brain structures that have been associated with olfactory function in previous structural and functional MRI studies,[16,137,138] the olfactory bulb is exclusively dedicated to olfaction. It receives and processes afferent odor information from olfactory receptor neurons, and then conveys this information directly to several subcortical and cortical regions without intermediary synapsing at the level of the thalamus.[106,139] Animal studies have also indicated a top-down neuro-modulatory cortical feedback to the olfactory bulb.[140] Thus, the close and direct link between the olfactory bulb and the other central components of the olfactory pathway is likely to underlie the strong associations between OBV, volumes of central olfactory structures and olfactory function.

Accumulating evidence suggests that early deficits in olfactory function are a frequent hallmark of many neurodegenerative diseases, and may serve both as a preclinical marker for cognitive impairment and a predictor of the rate of cognitive decline.[16,18]

Postmortem studies in patients with Alzheimer's and Parkinson's disease have demonstrated the presence of neurofibrillary tangles and alpha-synuclein aggregates, respectively, in both central olfactory regions,[141-143] and the olfactory bulb.[142-144] In fact, the olfactory bulb is among the first regions were these neuropathological changes occur.[142-144] Degeneration of olfactory bulb neurons and a lower volume of its glomerular component have also been reported in Alzheimer's and Parkinson's disease,[145,146] further corroborated by clinical evidence from imaging studies demonstrating smaller OBVs in patients compared to healthy controls.[114,147] Interestingly, in our study, OBV showed a stronger and more consistent relation to olfactory function compared to its central counterparts in the olfactory pathway and, in addition, largely mediated their association with olfactory function. Our findings therefore suggest that involvement of the olfactory bulb is likely to be one of the earliest underlying neuroanatomical substrates of age-associated olfactory dysfunction. In this light, OBV could thus be a clinically relevant quantitative marker of olfactory function that may prove useful in the identification of individuals at an increased risk of neurodegenerative disorders.

After accounting for the apparent indirect effects through the OBV, the direct relation between the volumes of central olfactory structures and olfactory function was more complex than previously reported. Notably, the association between hippocampal volume and olfactory function was strongly modified by age, albeit only in younger adults a statistically significant direct effect was found between hippocampal volume and odor identification. We observed a similar age-dependency of the direct effect for the amygdalar volume. These findings suggest that pathology of central olfactory structures, especially the hippocampus, in old age may also contribute to disturbed olfactory function perhaps through impaired odor memory.[4] Indeed, this age-dependent association may also explain some discrepancies in previous studies. For example, it was reported that in non-demented elderly the volumes of the amygdala, parahippocampal cortex and hippocampus were associated with odor identification,[16,137] while other studies failed to replicate these findings in younger individuals.[33,148] However, given the relatively large variability of the direct effect estimates, likely due to their stronger age-dependency, and the cross-sectional design of our study, future

longitudinal examinations involving larger groups of subjects across the entire age spectrum are required for more precise direct effect estimates.

In accordance with previous population-based studies, we found sex differences in odor identification.[120,149,150] Intriguingly, women outperformed men in odor identification ability, despite men having slightly larger OBVs even after adjustment for head size. This discrepancy may partly be due to endocrine differences between the sexes since odor sensitivity has been reported to vary with fluctuations of sex hormone levels in women.[151] Social behavior and learning efficiency may also play a role as, compared to men, women both tended to have a higher interest in the sense of smell[152] and had a larger improvement of their sensitivity to odorants with repeated test exposures.[153] These sex-differences could also have a neuroanatomical basis as women were found to have a higher number of both neurons and glial cells in their olfactory bulb, even after accounting for olfactory bulb mass,[154] underscoring the importance of sex-specific analyses in olfactory research.

Our study has several potential limitations. First, our analyses were based on cross-sectional data, limiting assessment of the temporal evolution of the olfactory structure/function relationships. Nevertheless, as the first large-scale study in the general population exploring the mutual interconnections between olfactory bulb, central olfactory structures and odor function, our findings provide a solid foundation for future longitudinal studies. Second, we used odor identification, a subtask of the complete olfactory testing battery, as a proxy for olfactory function. Compared to odor threshold and discrimination methods, testing for odor identification is less time consuming and more practical in both the general population and clinical settings.[123] Moreover, the odor identification test is extensively validated and widely used as a reliable screening test for olfactory dysfunction.[155] Third, the sequences of the brain MR scans were not specifically designed for optimal imaging of the olfactory bulb. However, our T2-weighted high-resolution images ($0.8 \times 0.8 \times 0.8$ mm^3) allowed for reliable and accurate detection of the olfactory bulb with low intra- and inter-rater variability.

In conclusion, our findings indicate that OBV is independently and robustly associated with odor identification in the general population and largely mediates the relation

between volumes of central olfactory structures and olfactory function. Given that olfactory dysfunction is a common and early feature of many neurodegenerative diseases, OBV may thus serve as a preclinical quantitative marker for the identification of individuals at an increased risk for developing these conditions in later life.

5. Insulin resistance accounts for metabolic syndrome-related alterations in brain structure

INTRODUCTION

Metabolic syndrome (MetS) is defined as a cluster of interconnected factors, including abdominal obesity, impaired glucose metabolism, elevated blood pressure and dyslipidemia. It is associated with an increased risk of cardiovascular diseases, diabetes mellitus type 2, stroke and dementia,[22,156,157] and thereby poses a major public health threat. Although MetS is likely to result from a complex interplay among different metabolic, vascular and inflammatory pathways, insulin resistance is thought to play an essential role in its pathogenesis.[158]

MetS and insulin resistance have been associated with changes in brain structure as assessed by magnetic resonance imaging (MRI). Many studies have focused on different components of the MetS,[22,159,160] yet the number of studies assessing the relation between MetS, insulin resistance and brain structural changes in the general population is limited. Most previous studies concerning MetS and insulin resistance enrolled patients in a clinical setting and mainly focused on macro- or micro-vascular changes, i.e. white matter hyperintensities, lacunes or stroke.[66-68] The few community- or population-based studies that investigated the relation between MetS or its components either utilized relatively rough global volumetric measures such as total brain volume (TBV), gray matter volume (GMV), white matter volume (WMV) or brain parenchymal fraction,[40,69-71] or exclusively focused on the medial temporal lobe structures, especially the hippocampus.[40,61] A few cohort studies used voxel-wise morphometry but these studies included relatively small groups of participants, usually confined to a restricted age range.[72,73,161]

It is still unclear to what extent the reported effects of MetS on brain structure are due to insulin resistance *per se*, or should be regarded as sequelae of its other components including obesity, dyslipidemia and hypertension. Elucidating this distinction at population level is important as it would imply a different prioritization of preventive and therapeutic strategies against the detrimental effects of MetS on the brain.

We aimed to *1)* assess the relation of MetS and insulin resistance − as measured by fasting serum insulin (FSI) and homeostatic model assessment of insulin resistance (HOMA-IR) - with structural brain changes, and *2)* evaluate to what extent insulin resistance could account for the pattern of structural brain changes seen in MetS.

RESEARCH DESIGN AND METHODS

Study design

This study is based on participants of the Rhineland Study, an ongoing population-based prospective cohort initiated in 2016 that enrolls participants aged 30 years and above at baseline from Bonn, Germany.[99] Approval to undertake the study was obtained from the ethics committee of the University of Bonn, Medical Faculty. The study was carried out in accordance with the recommendations of the International Conference on Harmonisation (ICH) Good Clinical Practice (GCP) standards (ICH-GCP). We obtained written informed consent from all participants in accordance with the Declaration of Helsinki.

Assessment of metabolic syndrome

Venous blood samples were collected after an overnight fast to determine the lipid, glucose and insulin levels. Fasting plasma glucose concentration was measured on the Nightingale platform (Nightingale Health, Helsinki, Finland).[103] FSI, triglyceride and HDL-C were measured using standard methods at the local clinical chemistry laboratory of the University Hospital of Bonn. HOMA-IR, which is highly correlated with direct estimates of insulin resistance as assessed by the hyperinsulinemic-euglycemic clamp technique,[162] was calculated using the following equation: HOMA-IR = (fasting glucose in mmol/L × fasting insulin in mIU/L)/22.5.[104] Waist circumference was measured in underwear with an anthropometric tape (SECA 201) by a trained technician to the nearest millimeter halfway between the 12th rib and the iliac crest. Blood pressure was measured three times with an oscillometric blood pressure device (OMRON 705 IT) in a semi-recumbent position, and the average of the second and third measurements was

calculated. The participants were asked to bring the medication that they used currently or during the last year for registration.

MetS was defined using the revised National Cholesterol Education Program Adult Treatment Panel III (NCEP-ATP III) criteria.[117,118] Participants were considered to have MetS if they met three or more of the following criteria: 1) waist circumference ≥ 102 cm in men and ≥ 88 cm in women, 2) triglyceride ≥ 150 mg/dl or treatment for hypertriglyceridemia, 3) HDL-C < 40 mg/dl in men and < 50 mg/dl in women or treatment for reduced HDL-C, 4) blood pressure ≥ 130/85 mmHg or on antihypertensive drug treatment, and 5) FPG ≥ 100 mg/dl or on drug treatment for elevated glucose.

MRI acquisition

MRI scans were collected on two 3T Siemens MAGNETOM Prisma MRI scanners (Siemens Healthcare, Erlangen, Germany) equipped with 64-channel head-neck coils in two examination sites in Bonn. The standardized protocol included a T1-weighted multi-echo magnetization-prepared rapid gradient-echo (MPRAGE) sequence[101] with 2D acceleration[100] (acquisition time = 6.5 min, 4 echoes, repetition time = 2560 ms, inversion time = 1100 ms, flip angle = 7°, matrix size = 320×320×224, voxel size = 0.8×0.8×0.8 mm^3), and a bandwidth-matched T2-weighted 3D Turbo-Spin-Echo (TSE) sequence using variable flip angles[133] (SPACE, acquisition time = 5 min, repetition time = 2800ms, echo time = 405ms, turbo factor = 282, matrix size = 320×320×224, voxel size = 0.8×0.8×0.8 mm^3). Both sequences utilize elliptical sampling[100] for faster acquisition.

MRI processing

We performed cortical reconstruction and volumetric segmentation with FreeSurfer image analysis suite version 6.0 (http://surfer.nmr.mgh.harvard.edu/) based on T1-weighted images.[163] A separate processing pipeline implemented in FreeSurfer based on T1- and T2-weighted images was used to obtain volumetric segmentation of the hippocampus and its subfields.[102] In this study, we examined global volumetric measures including TBV, WMV, subcortical and cortical GMV, and mean cortical thickness, as well as mean volumes of specific subcortical structures, i.e. amygdala,

hippocampus and its subfields. Each volumetric measure was adjusted for the Estimated Total Intracranial Volume (eTIV), an indicator of head size generated by FreeSurfer, by including it as a covariate in the model.

Vertex-wise analysis

The cortical reconstruction of each individual was used for whole brain vertex-wise (i.e. surface-based) analysis. We resampled the reconstructed brain cortical surface of each subject onto an average spherical surface through a spherical transformation. The cortical surface data of each subject was smoothed using a Gaussian kernel of 15-mm full width at half- maximum. Then, we performed a whole-brain vertex-wise analysis with a generalized linear model (GLM) *1)* to assess the effect of each predictor variable – i.e. FSI, HOMA-IR and MetS – on cortical thickness with age and sex as covariates, and *2)* to examine to what extent the MetS-related brain structural alteration could be explained by insulin resistance by additionally adjusting for FSI or HOMA-IR in GLM model of MetS. We corrected the GLM results for multiple comparisons using a false discovery rate (FDR) of 0.05,[164] and labeled them using the Desikan-Killiany-Tourville (DKT) atlas.[165] Only clusters larger than 200 mm^2 were reported and displayed on FreeSurfer's "fsaverage" brain in the results section.

Study population

For the present cross-sectional analysis, we used the data from the first 2000 participants enrolled in the Rhineland Study. In a subsample of 1158 of these subjects structural MRI scans were available. Participants with MRI scans were younger, had a lower waist circumference, had higher levels of high-density lipoprotein cholesterol (HDL-C) but lower levels of fasting plasma glucose (FPG), FSI and HOMA-IR, compared to those without a scan (**Table 5.1**). Among the 1158 participants, information for FSI, HOMA-IR and MetS was available for 1059, 1019, and 995 individuals respectively, with complete data on insulin resistance as assessed by FSI and HOMA-IR and MetS being available for 993 participants. Furthermore, 20 participants were excluded due to the presence of cerebral infarction or bleeding (n=12), intracranial tumor (n=5) or other parenchymal congenital or acquired defects (n=3) on brain imaging. Therefore, the

association between MetS, insulin resistance and brain structure were based on data from the remaining 973 participants.

Statistical analyses

Data are summarized as means (standard deviation, SD) or counts (percentage) for continuous and categorical variables, respectively. Differences between groups were compared using Student's t-test or multivariable linear regression for continuous variables, or Pearson's chi-square test for categorical variables. Separate multivariable linear regression models were used to examine the association between metabolic syndrome, insulin resistance and brain structural differences with adjustment for age, sex and head size (only for volumetric measures). Statistical significance was set at a two-tailed $p < 0.05$. All statistical analyses were performed using R version 3.4.[119]

Table 5.1 Characteristics of participants with and without MRI

Characteristic[1,2]	Without MRI	With MRI	Adjusted P value[3]
N	842	1158	
Age, year	57.6 (14.5)	52.9 (13.6)	<0.001
Women, n (%)	472 (56.1)	662 (57.2)	0.653
Waist circumference, cm	90.5 (14.8)	86.6 (12.5)	<0.001
Triglyceride, mg/dL	116.5 (75.1)	111.5 (72.1)	0.413
HDL-C, mg/dL	62.7 (18.1)	65.6 (18.9)	<0.001
Diastolic blood pressure, mmHg	77.0 (9.8)	76.9 (9.5)	0.408
Systolic blood pressure, mmHg	129.1 (17.2)	127.5 (15.9)	0.201
FPG, mmol/L	4.2 (1.0)	4.0 (0.6)	<0.001
FSI, mIU/L	10.8 (7.8)	9.7 (6.3)	0.015
HOMA-IR, unit	2.1 (1.9)	1.8 (1.4)	0.004

Abbreviations: HDL-C, High-density lipoprotein cholesterol; FPG, fasting plasma glucose; FSI, fasting serum insulin; HOMA-IR, homeostasis model assessment of insulin resistance.
[1] The characteristic was described as mean (SD) for continuous variables.
[2] Missing data in participants with and without MRI: waist circumference: 4 *vs.* 9; triglyceride and HDL-C: 98 *vs.* 97; blood pressure: 17 *vs.* 14; FPG: 58 *vs.* 50; FSI: 99 *vs.* 103; HOMA-IR: 139 *vs.* 131.
[3] Age- and sex-adjusted

RESULTS

General characteristics of the study population

Among the 973 participants, there were 354 (36.4%) with one, 159 (16.3%) with two, and 104 (10.7%) with three or more components of MetS, while 356 (36.6 %) of the participants had none of the MetS components. Overall, elevated blood pressure and waist circumference were the two most frequent components of MetS: More than half (51.0%) of the participants had elevated blood pressure defined as ≥ 130/85 mmHg or were on antihypertensive drug treatment (43.7% in women and 60.4% in men), and 23.2% (25.8% in women and 19.9% in men) had increased waist circumference. As shown in **Table 5.2**, individuals with MetS were on average older (mean difference [95% CI]: 6.5 [4.0, 9.0] years), more often male (53.8% *vs.* 42.1%), and had higher levels of fasting insulin and HOMA-IR (age- and sex-adjusted difference [95% CI]: 8.2 [7.0, 9.3] mIU/L for FSI, and 1.8 [1.6, 2.1] unit for HOMA-IR), and a worse metabolic status (age- and sex-adjusted difference [95% CI]: 16.8 [14.8, 18.7] cm for waist circumference, 104.7 [92.1, 117.3] mg/dL for triglyceride levels, -0.3 [-0.4, -0.3] mg/dL for HDL-C levels, 5.9 [4.0, 7.7] mmHg for diastolic blood pressure, 9.5 [6.6, 12.3] mmHg for systolic blood pressure, and 0.5 [0.4, 0.6] mmol/L for FPG levels) compared to those without MetS.

Table 5.2 Characteristics of participants with and without MetS

Characteristic[1]	Overall	With MetS	Without MetS
N	973	104	869
Age, year	52.5 (13.6)	58.3 (12.1)	51.8 (13.6)
Men, n (%)	422 (43.4)	56 (53.8)	366 (42.1)
Waist circumference, cm	86.6 (12.5)	103.7 (10.8)	84.6 (11.1)
Triglyceride, mg/dL	111.1 (71.4)	208.9 (108.1)	99.4 (55.1)
HDL-C, mg/dL	65.7 (18.8)	47.8 (11.6)	67.8 (18.4)
Diastolic blood pressure, mmHg [3]	77.3 (9.4)	83.3 (9.6)	76.5 (9.1)
Systolic blood pressure, mmHg [3]	127.9 (15.8)	139.9 (14.0)	126.5 (15.4)
FPG, mmol/L	4.0 (0.6)	4.5 (0.8)	3.9 (0.5)
FSI, mIU/L	9.6 (6.2)	17.1 (9.4)	8.8 (5.1)
HOMA-IR, unit	1.8 (1.3)	3.4 (2.0)	1.6 (1.0)

Abbreviations: MetS, metabolic syndrome; HDL-C, High-density lipoprotein cholesterol; FPG, fasting plasma glucose; FSI, fasting serum insulin; HOMA-IR, homeostasis model assessment of insulin resistance.

[1] The characteristic was described as mean (SD) for continuous variables.

[2] Missing data in participants with and without MetS: blood pressure: 2 *vs.* 7

Global volumetric measures

The regression-based estimates of the associations of MetS and insulin resistance with global volumetric brain MRI measures are summarized in **Table 5.3.** Higher FSI and HOMA-IR as well as the presence of MetS, were associated with a statistically significant reduction in cortical GMV and mean cortical thickness, and a statistically non-significant reduction in TBV. There were no obvious associations between MetS and insulin resistance indices and subcortical GMV and WMV.

Table 5.3 The association of MetS and insulin resistance with MRI global measures

	Difference (95% CI) in volume (mm^3)[1] or thickness (mm)[2]				
	TBV	WMV	Subcortical GMV	Cortical GMV	Mean cortical thickness
FSI (per SD)	-2788 (-5865, 288)	1074 (-906, 3054)	104 (-114, 322)	-2960*** (-4483, -1436)	-0.009** (-0.014, -0.003)
HOMA-IR (per SD)	-3305 (-6662, 52)	853 (-1309, 3014)	109 (-129, 347)	-3251*** (-4914, -1589)	-0.010*** (-0.016, -0.005)
MetS: with *vs.* without	-7923 (-16712, 865)	1689 (-3969, 7347)	108 (-514, 731)	-9157*** (-13502, -4811)	-0.030*** (-0.046, -0.015)

Abbreviations: FSI, fasting serum insulin; HOMA-IR, homeostasis model assessment of insulin resistance; MetS, metabolic syndrome; TBV, total brain volume; WMV, white matter volume; GMV, gray matter volume.
[1] Volumetric measures were adjusted for age, sex and head size assessed by the Estimated Total Intracranial Volume (eTIV).
[2] Mean cortical thickness was adjusted for age and sex.
** P<0.01; *** P<0.001

Volumes of amygdala, hippocampus and its subfields

As illustrated in **Table 5.4**, the degree of insulin resistance as evaluated by FSI and HOMA-IR and the presence of MetS were neither associated with the total volumes of the amygdala or the hippocampus, nor with hippocampal subfield volumes after adjustment for age, sex and head size.

Table 5.4 The association of insulin resistance and MetS with volumes of amygdala, hippocampus and its subfields

	Difference (95% CI) in the volume (mm^3)*												
	Amygdala	Hippocampus	Hippocampal subfields										
			para subiculum	pre subiculum	subiculum	CA1	CA2/3	CA4	GC-DG	HATA	fimbria	molecular layer	tail
FSI (per SD)	6.4 (-5.0, 17.7)	14.1 (-4.8, 33.0)	0.3 (-0.5, 1.1)	0.7 (-1.5, 2.8)	0.5 (-2.5, 3.5)	3.6 (-0.9, 8.2)	0.9 (-0.9, 2.7)	0.4 (-1.1, 1.9)	0.9 (-1.1, 2.8)	0.5 (-0.1, 1.0)	-0.1 (-1.4, 1.1)	2.7 (-0.6, 6.0)	3.8 (-0.5, 8.1)
HOMA-IR (per SD)	4.4 (-8.0, 16.7)	13.6 (-7.0, 34.3)	0.5 (-0.4, 1.3)	0.7 (-1.7, 3.1)	0.4 (-2.9, 3.6)	3.6 (-1.4, 8.5)	0.8 (-1.1, 2.8)	0.5 (-1.1, 2.1)	0.9 (-1.1, 3.0)	0.6 (0.0, 1.1)	-0.3 (-1.6, 1.1)	2.7 (-0.9, 6.3)	3.3 (-1.4, 7.9)
MetS: with *vs.* without	21.3 (-11.1, 53.7)	36.3 (-17.7, 90.2)	1.3 (-0.9, 3.5)	3.2 (-2.9, 9.4)	3.5 (-5.1, 12.1)	6.8 (-6.2, 19.8)	0.8 (-4.3, 5.9)	2.6 (-1.7, 6.9)	3.6 (-1.8, 9.1)	2.1 (0.6, 3.6)	0.1 (-3.4, 3.6)	3.6 (-5.9, 13.0)	8.7 (-3.6, 20.9)

Abbreviations: FSI, fasting serum insulin; HOMA-IR, homeostasis model assessment of insulin resistance; MetS, metabolic syndrome; CA, Cornu Ammonis; GC-DG: granule cell layer of dentate gyrus; HATA, hippocampal-amygdala-transition-area.
*Volumetric measures were adjusted for age, sex and head size assessed by the Estimated Total Intracranial Volume (eTIV).

Vertex-wise cortical thickness analysis

Whole brain vertex-wise associations between FSI, HOMA-IR and MetS and cortical thickness are summarized in **Figure 5.1** and **Table 5.5, 5.6** and **5.7**. The effects on cortical thickness of FSI, HOMA-IR and MetS exhibited a very similar pattern: The largest effect sizes were mainly located in the precentral cortex, transverse and superior temporal cortex, and the cuneus as well as its neighboring regions. Cortical thickness was substantially lower in those brain regions in which the effects of FSI, HOMA-IR and MetS overlapped (mean difference [95% CI] in cortical thickness between estimates in the overlapping and the non-overlapping regions: -0.0002 [-0.0003, -0.0001] mm for FSI, -0.0039 [-0.0040, -0.0038] mm for HOMA-IR, and -0.0067 [-0.0068, -0.0065] mm for MetS). Importantly, there was no independent effect of MetS on cortical thickness when the estimates were additionally adjusted for insulin resistance, as assessed by either FSI or HOMA-IR, in the whole brain analysis, i.e. for all brain regions the effect estimates became statistically non-significant after multiple comparison correction using FDR < 0.05.

Table 5.5 The association between FSI (per SD) and cortical thickness[1,2]

Hemisphere	Cluster size (mm^2)	Anatomical region[3]	Difference in cortical thickness (mm) per SD increase in FSI	Talairach coordinates		
				X	Y	Z
Left	5579	postcentral	-0.032	-53	-18	32
	1428	postcentral	-0.032	-53	-18	32
	997	superior temporal	-0.025	-64	-29	4
	809	supramarginal	-0.030	-53	-20	30
	645	precentral	-0.023	-50	-6	8
	546	lateral occipital	-0.019	-40	-75	-7
	524	lingual	-0.020	-22	-53	6
	491	precentral	-0.034	-34	-21	50
	400	lingual	-0.020	-26	-45	-3
	300	paracentral	-0.018	-6	-13	47
Right	4375	superior temporal	-0.031	34	0	-18
	2774	superior temporal	-0.031	34	0	-18
	481	middle temporal	-0.019	48	-13	-15
	438	insula	-0.029	40	-14	-9
	3512	precentral	-0.039	35	-19	52
	2197	precentral	-0.039	35	-19	52
	792	caudal middle frontal	-0.027	43	4	42
	369	paracentral	-0.030	5	-23	68
	1048	cuneus	-0.019	4	-73	26
	425	parsopercularis	-0.019	50	15	16
	416	entorhinal	-0.032	23	-14	-25
	380	fusiform	-0.020	38	-69	-8
	297	superior frontal	-0.021	8	4	51
	223	parstriangularis	-0.018	44	23	6

[1] Regions that survived a cluster-wise correction for multiple comparisons using FDR< 0.05 and exceeding 200 mm^2 are reported.
[2] Main regions (>10% of the cluster size) in the cluster larger than 2000 mm^2 were given.
[3] Regions were labeled using the Desikan-Killiany-Tourville atlas.

Table 5.6 The association between HOMA-IR (per SD) and cortical thickness[1,2]

Hemisphere	Cluster size (mm^2)	Anatomical region[3]	Difference in cortical thickness (mm) per SD increase in HOMA-IR	Talairach coordinates		
				X	Y	Z
Left	10127	precentral	-0.040	-34	-21	50
	2326	precentral	-0.040	-34	-21	50
	1733	postcentral	-0.034	-53	-18	33
	1412	superior temporal	-0.028	-64	-30	5
	1065	supramarginal	-0.031	-53	-20	30
	1443	lingual	-0.022	-22	-53	5
	1297	lateral occipital	-0.022	-36	-78	-8
	672	fusiform	-0.023	-29	-40	-15
	559	superior temporal	-0.032	-36	5	-27
	396	lateral occipital	-0.018	-41	-76	1
	279	superior frontal	-0.020	-20	7	53
	274	superior parietal	-0.017	-20	-59	47
Right	12717	precentral	-0.049	35	-19	51
	3139	superior temporal	-0.034	33	-1	-20
	3115	precentral	-0.049	35	-19	51
	2849	parahippocampal	-0.026	20	-32	-9
	974	cuneus	-0.023	6	-72	25
	573	lingual	-0.025	16	-51	-3
	500	precuneus	-0.020	18	-53	16
	430	pericalcarine	-0.019	8	-64	15
	787	fusiform	-0.024	39	-69	-8
	431	postcentral	-0.025	54	-14	36
	396	lateral occipital	-0.019	44	-70	7
	243	middle temporal	-0.022	50	-48	10

[1] Regions that survived a cluster-wise correction for multiple comparisons using FDR< 0.05 and exceeding 200 mm^2 are reported.
[2] Main regions (>10% of the cluster size) in the cluster larger than 2000 mm^2 were given.
[3] Regions were labeled using the Desikan-Killiany-Tourville atlas.

Table 5.7 The association between MetS and cortical thickness[1,2]

Hemisphere	Cluster size (mm^2)	Anatomical region[3]	Difference in cortical thickness (mm)	Talairach coordinates		
				X	Y	Z
Left	11096	postcentral	-0.086	-43	-17	18
	3546	precentral	-0.084	-55	3	31
	3049	superior frontal	-0.075	-10	33	46
	1179	postcentral	-0.086	-43	-17	18
	4519	transverse temporal	-0.082	-49	-21	7
	1414	inferior parietal	-0.067	-42	-51	37
	1367	superior temporal	-0.074	-52	-20	2
	957	supramarginal	-0.067	-42	-50	36
	4048	fusiform	-0.083	-40	-70	-8
	1439	lateral occipital	-0.079	-40	-71	-5
	1022	middle temporal	-0.081	-60	-51	2
	818	fusiform	-0.083	-40	-70	-8
	690	inferior temporal	-0.065	-39	-62	-2
	1904	pericalcarine	-0.056	-13	-72	6
	240	rostral middle frontal	-0.045	-39	39	22
	208	superior parietal	-0.052	-19	-61	52
Right	15132	paracentral	-0.095	5	-23	68
	3211	precentral	-0.095	5	-24	68
	1998	superior temporal	-0.071	49	5	-16
	1625	lingual	-0.074	18	-54	-3
	1227	fusiform	-0.080	44	-67	-9
	1114	superior frontal	-0.063	12	59	-10
	548	middle temporal	-0.056	64	-24	-10
	372	isthmus cingulate	-0.049	7	-33	33
	341	middle temporal	-0.050	45	-60	7
	330	superior frontal	-0.057	22	4	53
	301	supramarginal	-0.051	53	-37	42
	251	precuneus	-0.046	6	-64	36

[1] Regions that survived a cluster-wise correction for multiple comparisons using FDR< 0.05 and exceeding 200 mm^2 are reported.
[2] Main regions (>10% of the cluster size) in the cluster larger than 2000 mm^2 were given.
[3] Regions were labeled using the Desikan-Killiany-Tourville atlas.

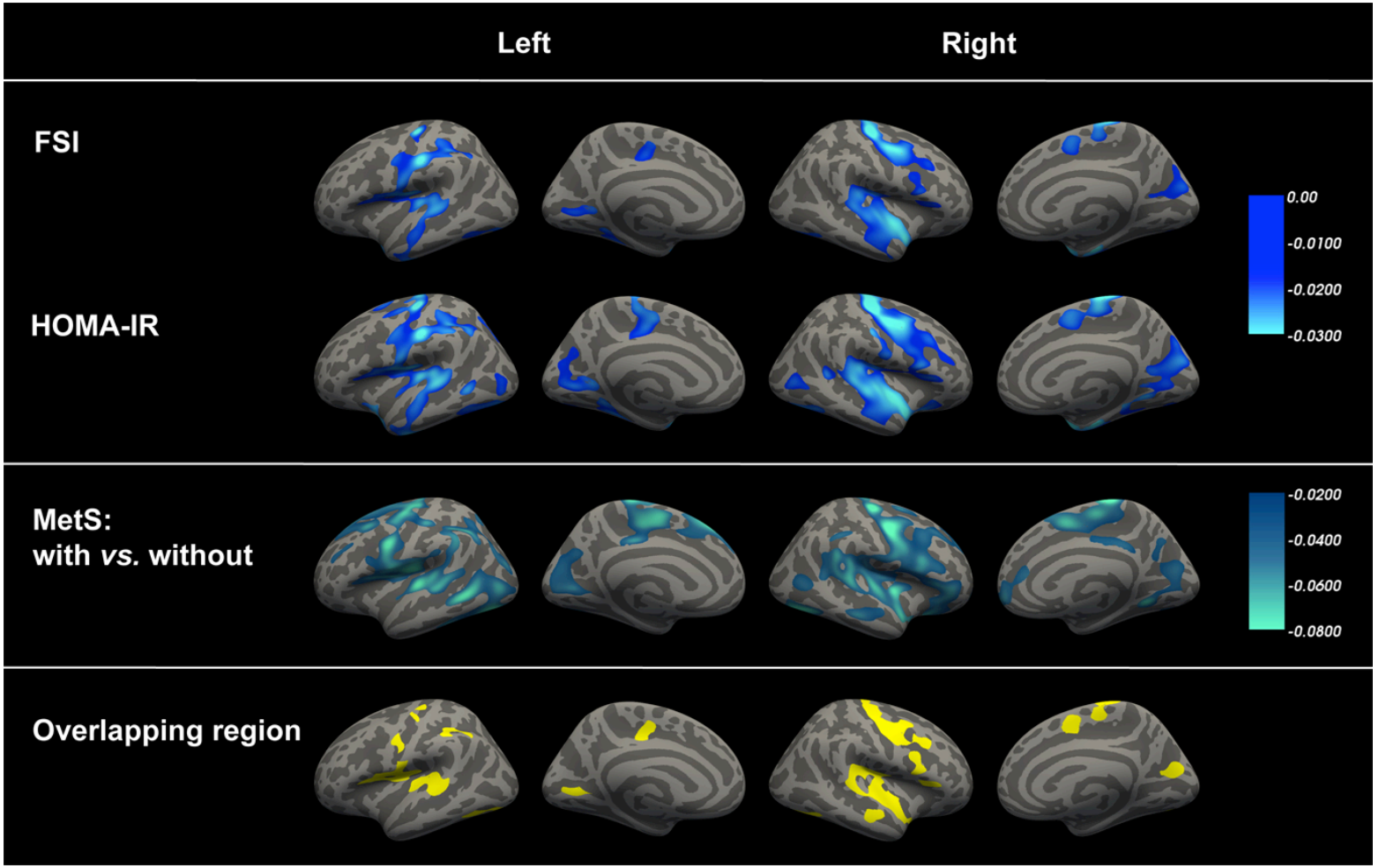

Figure 5.1 The relation between insulin resistance, metabolic syndrome and cortical thickness.
Vertex-based whole brain analysis in 973 participants (aged 30 years and above) demonstrated an inverse association between insulin resistance as represented by fasting serum insulin (FSI) and homeostasis model assessment of insulin resistance (HOMA-IR) as well as metabolic syndrome (MetS) and cortical thickness in several brain regions. All clusters that survived statistical significance testing after multiple comparisons correction using FDR <0.05 and were larger than 200 mm2 are illustrated. The color scales indicate the age- and sex-adjusted beta values per standard deviation increase in FSI or HOMA-IR or between participants with and without MetS.

DISCUSSION

In this large-scale population-based study, we found that both MetS and insulin resistance were associated with a reduced cortical GMV and mean cortical thickness but not with WMV or with volumes of subcortical gray matter structures, including the amygdala, the hippocampus or its subfields. In addition, by applying vertex-wise whole brain analysis, we showed that the effects of MetS and insulin resistance on cortical thickness exhibited a remarkable degree of similarity, with the most pronounced effects occurring in the precentral cortex, transverse and superior temporal cortex, as well as the cuneus and its neighboring regions.

A negative association of fasting insulin, HOMA-IR or MetS with global measures of brain structural integrity, such as TBV and brain parenchymal fraction, has been described before in relatively small-scaled studies.[40,71] However, only few studies investigated the effects of these metabolic indices on specific brain compartments, including gray matter, white matter and cortical and subcortical structures in the general population. Studies in selected cohorts have so far yielded conflicting results: An inverse relation between HOMA-IR and both GMV and WMV was reported in elderly adults,[72] while in elderly participants from long-lived families no association was found between insulin sensitivity or MetS and gray and white matter volumes.[69,166] We found that in the general population, the presence of MetS as well as higher FSI and HOMA-IR values are associated with smaller TBV, with the effect being mainly attributable to the influence on cortical gray matter, either assessed through volume or thickness, rather than on white matter or subcortical gray matter.

To pinpoint the cortical regions affected by MetS and insulin resistance more precisely, we applied whole-brain vertex-based morphometry, which demonstrated a considerable degree of similarity in the spatial patterns of cortical thinning in relation to MetS, FSI and HOMA-IR. Moreover, the areas in which the effects of MetS and insulin resistance overlapped - i.e. the precentral cortex, transverse and superior temporal cortex, and cuneus and its neighboring regions - exhibited the largest reduction of cortical thickness and coincided with the regions that have been associated with HOMA-IR previously.[72,73] To the best of our knowledge, the present study is the first to assess brain morphology

in relation to both MetS and insulin resistance simultaneously. Given the substantial spatial overlap between the effects of MetS and insulin resistance on brain structure, as well as the fact that no independent effect of MetS remained on cortical thickness after adjustment for insulin resistance, our findings suggest that insulin resistance is the core mediator responsible for the central nervous system effects of MetS.

Many studies have indeed found a higher prevalence of deficits in multiple cognitive domains in subjects with insulin resistance and MetS.[21,22,167] Interestingly, in our study, the pattern of cortical thinning associated with both insulin resistance and MetS approximately corresponded to the regions mainly involved in motor regulation and auditory and visual information processing. We found no association with structural changes in areas associated with higher cognitive functions as for example language processing or executive function. It remains unclear to what extent impairments in other functions that are required to perform most cognitive tests, including motor dexterity as well as hearing and visual function, might actually underlie the negative association between cognitive function and insulin resistance or MetS. The associations between central motor, auditory or visual processing and insulin resistance and MetS have received little study, especially in the general population.[168,169] Thus, our findings warrant further assessment of the role of motor function and auditory and visual processing as mediators of the well-established association between cognitive function and insulin resistance and MetS.

Given the high prevalence of cognitive dysfunction in patients with insulin resistance and MetS, several previous MRI studies have focused on the role of the hippocampus; however, the ensuing results have been inconsistent. MetS has been associated with higher hippocampal volume at baseline in patients with multiple-domain mild cognitive impairment.[170] Conversely, in individuals at risk of Alzheimer's disease, insulin resistance was reported to be inversely linked to hippocampal and parahippocampal volume at baseline as well as progressive atrophy over time.[73] However, two other large population-based cohort studies failed to replicate this association using manually traced volumetric measures of the hippocampus.[40,61] In the current work, state-of-the-art automated hippocampal segmentation not only enabled exploration of the association of insulin resistance and MetS with the overall hippocampal volume, but also allowed for

further detailed assessment of potential effects on the hippocampal subfields. In accord with previous population-based studies, we found no association between insulin resistance or MetS and hippocampal volume. In addition, we extended these findings by demonstrating that there is also no relation between insulin resistance or MetS and volumes of hippocampal subfields.

The strengths of this study include its large sample size, the wide age range (i.e. 30 - 95 years), that it is population-based, and the availability of data on both MetS and insulin resistance. However, our study also has limitations. First, we used cross-sectional observational data, which limits making inferences regarding the directionality of the effects between metabolic indices and brain structural measures. Nevertheless, we consider it unlikely that the cortical thinning induced the metabolic disturbances. Moreover, we could not assess the effects of the duration of MetS or insulin resistance on brain structure. Finally, the prevalence of MetS was relative low (i.e. 10.7%) in our cohort as compared to previous studies,[125-127] which may be due to the relatively large proportion of young adult participants in the Rhineland Study.

In conclusion, we found that both MetS and insulin resistance were linked to reduced cortical gray matter volume and thickness, especially in regions involved in motor regulation and auditory and visual signal processing, but not to volumetric changes in subcortical brain regions or the hippocampal or amygdala area. Furthermore, we found that the effect of MetS on brain structure was largely accounted for by insulin resistance, implying that insulin resistance underlies MetS-related cortical brain atrophy. This suggests that screening for and early intervention on insulin resistance could be a viable path to preventing brain atrophy related to metabolic syndrome.

6. General discussion

The objective of this thesis was to gain greater insight in associations between MetS metabolic syndrome, brain structure -in particular olfactory brain structures-, and olfactory function. In this chapter, I will summarize and review the main findings, discuss some methodological considerations and give directions for further research.

To gain a better understanding of how MetS influences olfaction, in **Chapter 3** we assessed the association of MetS and its pathophysiologically major component insulin resistance, with olfactory structures and function. To this end, I first developed a reliable manual segmentation protocol of olfactory bulb (**Chapter 2**), and implemented it in the Rhineland Study. The manually labeled data was used in the subsequent analyses. In our population, we observed that MetS and insulin resistance were associated with volumes of several odor-related brain cortical structures, including entorhinal cortex, insula, and lateral and medial orbitofrontal cortex. In addition, based on a subsample with manually segmented OBVs, a negative association between MetS as well as insulin resistance and OBV was also observed, albeit not statistically significant. Our findings are in line with and extend previous reports, which described associations of the insula and particularly the orbitofrontal cortex with some of MetS components and insulin resistance.[44,50,54,58,59,73] Although a higher prevalence of self-reported olfactory dysfunction was reported in individuals with MetS compared to those without in limited population-based studies,[9,10] we failed to find an association between MetS and objectively assessed olfactory function. Given that no population-based study so far investigated the relationship between metabolic syndrome and objective olfactory function, additional studies are required before a more definitive link can be established. Moreover, the different associations of MetS and insulin resistance with olfactory structures and function highlight the importance of a systematic assessment of olfactory structural-functional relationship in the general population.

Consequently, in **Chapter 4**, we evaluated the associations of olfactory brain structures with olfactory function. Olfactory dysfunction is a prodromal manifestation of cognitive impairment and several neurodegenerative disorders,[11,13-16] and several pathological

proteins, i.e. α-synuclein, hyperphosphorylated tau protein, and neurofilament, are deposited in the olfactory bulb prior to other central odor-related structures.[129,142-144] Therefore, we further examined the relative contributions of olfactory bulb and central odor structures to olfactory function. In line with previous small-scale studies,[31,33,114,147] OBV was positively associated with olfactory function assessed by SIT-12 in the general population. Compared to its central counterparts, the association between OBV and olfactory function was much stronger and less influenced by aging. More importantly, we demonstrated a mediatory role of OBV in the association between the volumes of central olfactory structures and olfactory function, which suggests a likely early involvement of the olfactory bulb in the olfactory dysfunction.

In **Chapter 5**, we investigated the association of MetS and insulin resistance with whole-brain morphology, rather than with predefined region of interests. Although MetS and insulin resistance has been inversely associated with TBV or brain parenchymal ratio in cohort studies,[40,70,71] their effects on specific brain compartments, including white matter, subcortical and cortical gray matter, remain unclear.[69,72,166] In accordance with previous findings, we found that the presence of MetS and higher values of FSI and HOMA-IR were associated with smaller TBV. Additionally, this effect was mainly attributable to their influence on cortical gray matter, rather than on white matter or subcortical gray matter. Limited voxel-based MRI studies found that MetS and insulin resistance were associated with several brain regions, such as superior and middle temporal gyrus, insula, and prefrontal gyrus.[72-74] However, to the best of our knowledge, no population-based study so far has evaluated brain morphology in relation to both MetS and insulin resistance simultaneously. In the current work, we compared spatial patterns of cortical thinning associated with MetS and insulin resistance and observed a remarkable degree of similarity. Moreover, no significant effect of MetS on cortical thickness was found after adjustment for either FSI or HOMA-IR. Thus, our findings suggest that insulin resistance is the underlying factor of MetS-related structural changes in the brain. We also noticed that the insulin resistance- and MetS-related cortical thinning was located approximately in regions involved in motor regulation, and auditory and visual processing, which are three processes commonly involved in cognitive tests. This finding is worthy of further investigation since MetS is frequently associated with cognitive dysfunction.[19-21]

All the studies described in this thesis are embedded in the Rhineland Study, a prospective population-based cohort study. By sampling from the population registry of residents, the study design aims to reflect the distribution of sex, age, and other factors of a general adult population, thereby enhancing the generalizability of our results. However, we only used cross-sectional data from the baseline examinations, which limits the inference of causality. In addition, older participants with a worse health condition were more likely to be excluded from the MRI study. Olfactory function in our study relied on a brief version of odor identification test, an established olfactory test that is widely used.[105] Although it was suggested that results from most olfactory psychophysical tests were correlated with one another,[124] a more detailed test of olfactory function could still improve the evaluation of olfactory function,[171] and help distinguish different involvement of odor-related structures in each subtask.[33] In addition, the overall prevalence of MetS was 12.6% in the first 2000 participants from the Rhineland study, which is relatively low compared to other studies in Europe.[125-127] This may have partly been due to demographic characteristics of the residents in Bonn, and a relatively large proportion of young adult participants enrolled in the study. It would be helpful to confirm our findings in other population-based studies.

Our work provides several implications for future studies. We found that MetS and insulin resistance was associated with several olfactory brain cortical structures but not with olfactory function. As accumulative evidence from both human and animal studies has suggested metabolic disturbance could influence the olfactory function,[5] it would be of interest to investigate this topic further. Population-based research with a large sample size, a wide age range, high-resolution MRI scans, a more complete olfactory test battery, and repeated measurements, is needed to establish the link between MetS and olfaction both structurally and functionally. We observed a unique intermediary role of the olfactory bulb in the olfactory pathway. Unlike other central odor-related structures, the olfactory bulb is exclusively dedicated to olfaction, and is early involved in several neuropathological processes.[129,142-144] Therefore, more attention should be paid to this tiny structure in the forebrain, which was hitherto mostly neglected in human MRI studies, even in studies of olfaction. To ensure a reproducible, reliable and time-efficient measurement of OBV in a large population-based cohort, an automated segmentation

method is definitely required. Although our current work on deep-learning method showed promising results, several issues remain to be addressed: aplasia of the olfactory bulb, inhomogeneous intensity within the olfactory bulb, and a proper evaluation of the performance of a deep-learning model, i.e. Dice score and age- and sex-dependency of OBV shown in the manual segmentation. Further investigation in longitudinal studies is also needed to confirm the temporal sequence of the involvement of olfactory structures that has been indicated in animal studies.[18] The close relation of MetS with cardio-metabolic diseases and dementia[22,156,157] emphasizes the importance of its prevention and monitoring. Our findings suggested that insulin resistance is an underlying factor of MetS-related brain morphological alteration. Since both FSI and HOMA-IR are easily accessible, their potential utility should be further evaluated in future interventional and longitudinal studies.

Although much of this thesis is in terms of the metabolic influence on olfactory function, we recognize that effects may also exist in the opposite direction. It is thought that olfactory function affects metabolism through food-related behaviors. Although exposure to food-cue odors stimulates appetite,[172,173] induces neural physiological actions,[174,175] and cephalic phase responses,[176-178] it does not always reflect in actual food intake.[179-181] Therefore, it remains unclear whether and how the olfactory system influences metabolism. A recent study in mice provides new insights into odor-induced metabolic activity.[6] They observed that ablation of olfactory sensory neurons did not alter food intake, but increased energy expenditure by promoting lipolysis and thermogenesis and browning of adipose tissue. Furthermore, mice with enhanced smell sensitivity exhibited increased adiposity, hyperinsulinaemia and insulin resistance. However, since the human olfactory system differs from that of rodents and other mammals,[182] it is unclear to what extent these observations in mice are relevant for understanding human biology.

7. Abstract

Both MetS and olfactory dysfunction are highly prevalent disorders, and closely related to brain function. Although several studies implied a link between several components of MetS and olfactory dysfunction, it remains unclear how MetS influences olfactory function. Furthermore, the neuroanatomical basis of neither MetS nor olfactory dysfunction is well understood in the general population. Therefore, based on the first 2000 participants from the Rhineland Study, a population-based cohort, we aimed to elucidate the relations between metabolic syndrome, brain structure, and olfactory function. MetS was defined in accordance with revised criteria of National Cholesterol Education Program Adult Treatment Panel III. Brain structures were assessed on high-resolution T1- and T2-weighted brain images at 3 Tesla. Performance on the 12-item "Sniffin' Sticks" odor identification test was used as a proxy of olfactory function. For this thesis, I first systematically examined the relation of MetS and insulin resistance with both olfactory brain structures and function. I found that MetS and insulin were associated with several olfactory brain structures, i.e. entorhinal cortex, insula, and lateral and medial orbitofrontal cortex, but not with objectively quantified olfactory function. Subsequently, I further investigated the association between olfactory brain structures and olfactory function. I found that olfactory bulb volume (OBV) was not only consistently associated with olfactory function, but also with several central odor-related structures across all age groups. Moreover, OBV played a mediatory role in the association between volumes of central olfactory structures and olfactory function. Finally, I examined the relation between MetS and insulin resistance and brain morphology using vertex-based analyses. I observed that MetS and insulin resistance are related with a very similar spatial pattern of brain cortical thinning. Additionally, insulin resistance accounted for most of the MetS-related brain alterations. In conclusion, the work described in this thesis provides new evidence for the association of MetS and insulin resistance with olfaction, and sheds light upon the neuroanatomical correlates of both olfactory function and MetS.

8. List of figures

9. List of tables

10. References

1. Saklayen MG. The Global Epidemic of the Metabolic Syndrome. *Curr Hypertens Rep.* 2018;20(2):12.

2. Murphy C, Schubert CR, Cruickshanks KJ, Klein BE, Klein R, Nondahl DM. Prevalence of olfactory impairment in older adults. *JAMA.* 2002;288(18):2307-2312.

3. Boesveldt S, Lindau ST, McClintock MK, Hummel T, Lundstrom JN. Gustatory and olfactory dysfunction in older adults: a national probability study. *Rhinology.* 2011;49(3):324-330.

4. Gouveri E, Katotomichelakis M, Gouveris H, Danielides V, Maltezos E, Papanas N. Olfactory dysfunction in type 2 diabetes mellitus: an additional manifestation of microvascular disease? *Angiology.* 2014;65(10):869-876.

5. Palouzier-Paulignan B, Lacroix MC, Aime P, et al. Olfaction under metabolic influences. *Chem Senses.* 2012;37(9):769-797.

6. Riera CE, Tsaousidou E, Halloran J, et al. The Sense of Smell Impacts Metabolic Health and Obesity. *Cell Metab.* 2017;26(1):198-211 e195.

7. Savigner A, Duchamp-Viret P, Grosmaitre X, et al. Modulation of spontaneous and odorant-evoked activity of rat olfactory sensory neurons by two anorectic peptides, insulin and leptin. *J Neurophysiol.* 2009;101(6):2898-2906.

8. Tong J, Mannea E, Aime P, et al. Ghrelin enhances olfactory sensitivity and exploratory sniffing in rodents and humans. *J Neurosci.* 2011;31(15):5841-5846.

9. Hwang SH, Kang JM, Seo JH, Han KD, Joo YH. Gender Difference in the Epidemiological Association between Metabolic Syndrome and Olfactory Dysfunction: The Korea National Health and Nutrition Examination Survey. *PLoS One.* 2016;11(2):e0148813.

10. Park DY, Kim HJ, Kim CH, Lee JY, Han K, Choi JH. Prevalence and relationship of olfactory dysfunction and tinnitus among middle- and old-aged population in Korea. *PLoS One.* 2018;13(10):e0206328.

11. Doty RL. Olfactory dysfunction in neurodegenerative diseases: is there a common pathological substrate? *Lancet Neurol.* 2017;16(6):478-488.

12. Hummel T, Whitcroft KL, Andrews P, et al. Position paper on olfactory dysfunction. *Rhinology.* 2016;56(1):1-30.

13. Roberts RO, Christianson TJ, Kremers WK, et al. Association Between Olfactory Dysfunction and Amnestic Mild Cognitive Impairment and Alzheimer Disease Dementia. *JAMA Neurol.* 2016;73(1):93-101.

14. Miller DB, O'Callaghan JP. Biomarkers of Parkinson's disease: present and future. *Metabolism.* 2015;64(3 Suppl 1):S40-46.

15. Schubert CR, Carmichael LL, Murphy C, Klein BE, Klein R, Cruickshanks KJ. Olfaction and the 5-year incidence of cognitive impairment in an epidemiological study of older adults. *J Am Geriatr Soc.* 2008;56(8):1517-1521.

16. Dintica CS, Marseglia A, Rizzuto D, et al. Impaired olfaction is associated with cognitive decline and neurodegeneration in the brain. *Neurology.* 2019;92(7):e700-e709.

17. Sohrabi HR, Bates KA, Weinborn MG, et al. Olfactory discrimination predicts cognitive decline among community-dwelling older adults. *Transl Psychiatry.* 2012;2:e118.

18. Rey NL, Wesson DW, Brundin P. The olfactory bulb as the entry site for prion-like propagation in neurodegenerative diseases. *Neurobiol Dis.* 2018;109(Pt B):226-248.

19. Komulainen P, Lakka TA, Kivipelto M, et al. Metabolic syndrome and cognitive function: a population-based follow-up study in elderly women. *Dement Geriatr Cogn Disord.* 2007;23(1):29-34.

20. Ng TP, Feng L, Nyunt MS, et al. Metabolic Syndrome and the Risk of Mild Cognitive Impairment and Progression to Dementia: Follow-up of the Singapore Longitudinal Ageing Study Cohort. *JAMA Neurol.* 2016;73(4):456-463.

21. Ekblad LL, Rinne JO, Puukka P, et al. Insulin Resistance Predicts Cognitive Decline: An 11-Year Follow-up of a Nationally Representative Adult Population Sample. *Diabetes Care.* 2017;40(6):751-758.

22. Yates KF, Sweat V, Yau PL, Turchiano MM, Convit A. Impact of metabolic syndrome on cognition and brain: a selected review of the literature. *Arterioscler Thromb Vasc Biol.* 2012;32(9):2060-2067.

23. Miranda PJ, DeFronzo RA, Califf RM, Guyton JR. Metabolic syndrome: definition, pathophysiology, and mechanisms. *Am Heart J.* 2005;149(1):33-45.

24. Wilson DA, Chapuis J, Sullivan RM. Cortical Olfactory Anatomy and Physiology. In: Doty R, ed. *Handbook of olfaction and gustation.* 3rd ed. New York, US: Wiley-Liss; 2015:209-226.

25. Ghatpande AS, Reisert J. Olfactory receptor neuron responses coding for rapid odour sampling. *J Physiol.* 2011;589(Pt 9):2261-2273.

26. Han P, Whitcroft KL, Fischer J, et al. Olfactory brain gray matter volume reduction in patients with chronic rhinosinusitis. *Int Forum Allergy Rhinol.* 2017;7(6):551-556.

27. Bitter T, Siegert F, Gudziol H, et al. Gray matter alterations in parosmia. *Neuroscience.* 2011;177:177-182.

28. Yao L, Yi X, Pinto JM, et al. Olfactory cortex and Olfactory bulb volume alterations in patients with post-infectious Olfactory loss. *Brain Imaging Behav.* 2018;12(5):1355-1362.

29. Peng P, Gu H, Xiao W, et al. A voxel-based morphometry study of anosmic patients. *Br J Radiol.* 2013;86(1032):20130207.

30. Karstensen HG, Vestergaard M, Baare WFC, et al. Congenital olfactory impairment is linked to cortical changes in prefrontal and limbic brain regions. *Brain Imaging Behav.* 2018;12(6):1569-1582.

31. Buschhuter D, Smitka M, Puschmann S, et al. Correlation between olfactory bulb volume and olfactory function. *Neuroimage.* 2008;42(2):498-502.

32. Shen J, Kassir MA, Wu J, et al. MR volumetric study of piriform-cortical amygdala and orbitofrontal cortices: the aging effect. *PLoS One.* 2013;8(9):e74526.

33. Seubert J, Freiherr J, Frasnelli J, Hummel T, Lundstrom JN. Orbitofrontal cortex and olfactory bulb volume predict distinct aspects of olfactory performance in healthy subjects. *Cereb Cortex.* 2013;23(10):2448-2456.

34. Debette S, Wolf C, Lambert JC, et al. Abdominal obesity and lower gray matter volume: a Mendelian randomization study. *Neurobiol Aging.* 2014;35(2):378-386.

35. Debette S, Beiser A, Hoffmann U, et al. Visceral fat is associated with lower brain volume in healthy middle-aged adults. *Ann Neurol.* 2010;68(2):136-144.

36. Brooks SJ, Benedict C, Burgos J, et al. Late-life obesity is associated with smaller global and regional gray matter volumes: a voxel-based morphometric study. *Int J Obes (Lond).* 2013;37(2):230-236.

37. Falvey CM, Rosano C, Simonsick EM, et al. Macro- and microstructural magnetic resonance imaging indices associated with diabetes among community-dwelling older adults. *Diabetes Care.* 2013;36(3):677-682.

38. Saczynski JS, Siggurdsson S, Jonsson PV, et al. Glycemic status and brain injury in older individuals: the age gene/environment susceptibility-Reykjavik study. *Diabetes Care.* 2009;32(9):1608-1613.

39. de Bresser J, Tiehuis AM, van den Berg E, et al. Progression of cerebral atrophy and white matter hyperintensities in patients with type 2 diabetes. *Diabetes Care.* 2010;33(6):1309-1314.

40. Tan ZS, Beiser AS, Fox CS, et al. Association of metabolic dysregulation with volumetric brain magnetic resonance imaging and cognitive markers of subclinical brain aging in middle-aged adults: the Framingham Offspring Study. *Diabetes Care.* 2011;34(8):1766-1770.

41. Wiseman RM, Saxby BK, Burton EJ, Barber R, Ford GA, O'Brien JT. Hippocampal atrophy, whole brain volume, and white matter lesions in older hypertensive subjects. *Neurology.* 2004;63(10):1892-1897.

42. Firbank MJ, Wiseman RM, Burton EJ, Saxby BK, O'Brien JT, Ford GA. Brain atrophy and white matter hyperintensity change in older adults and relationship to blood pressure. Brain atrophy, WMH change and blood pressure. *J Neurol.* 2007;254(6):713-721.

43. Wolf H, Hensel A, Arendt T, Kivipelto M, Winblad B, Gertz HJ. Serum lipids and hippocampal volume: the link to Alzheimer's disease? *Ann Neurol.* 2004;56(5):745-748.

44. Walther K, Birdsill AC, Glisky EL, Ryan L. Structural brain differences and cognitive functioning related to body mass index in older females. *Hum Brain Mapp.* 2010;31(7):1052-1064.

45. Raji CA, Ho AJ, Parikshak NN, et al. Brain structure and obesity. *Hum Brain Mapp.* 2010;31(3):353-364.

46. Raffield LM, Cox AJ, Freedman BI, et al. Analysis of the relationships between type 2 diabetes status, glycemic control, and neuroimaging measures in the Diabetes Heart Study Mind. *Acta Diabetol.* 2016;53(3):439-447.

47. Moran C, Phan TG, Chen J, et al. Brain atrophy in type 2 diabetes: regional distribution and influence on cognition. *Diabetes Care.* 2013;36(12):4036-4042.

48. Moran C, Munch G, Forbes JM, et al. Type 2 diabetes, skin autofluorescence, and brain atrophy. *Diabetes.* 2015;64(1):279-283.

49. Chen Z, Li L, Sun J, Ma L. Mapping the brain in type II diabetes: Voxel-based morphometry using DARTEL. *Eur J Radiol.* 2012;81(8):1870-1876.

50. Raz N, Rodrigue KM, Kennedy KM, Acker JD. Vascular health and longitudinal changes in brain and cognition in middle-aged and older adults. *Neuropsychology.* 2007;21(2):149-157.

51. Ward MA, Bendlin BB, McLaren DG, et al. Low HDL Cholesterol is Associated with Lower Gray Matter Volume in Cognitively Healthy Adults. *Front Aging Neurosci.* 2010;2.

52. Taki Y, Kinomura S, Sato K, et al. Relationship between body mass index and gray matter volume in 1,428 healthy individuals. *Obesity (Silver Spring).* 2008;16(1):119-124.

53. Jongen C, van der Grond J, Kappelle LJ, et al. Automated measurement of brain and white matter lesion volume in type 2 diabetes mellitus. *Diabetologia.* 2007;50(7):1509-1516.

54. Kumar A, Haroon E, Darwin C, et al. Gray matter prefrontal changes in type 2 diabetes detected using MRI. *J Magn Reson Imaging.* 2008;27(1):14-19.

55. Brundel M, van den Heuvel M, de Bresser J, Kappelle LJ, Biessels GJ, Utrecht Diabetic Encephalopathy Study G. Cerebral cortical thickness in patients with type 2 diabetes. *J Neurol Sci.* 2010;299(1-2):126-130.

56. Whalley LJ, Staff RT, Murray AD, et al. Plasma vitamin C, cholesterol and homocysteine are associated with grey matter volume determined by MRI in non-demented old people. *Neurosci Lett.* 2003;341(3):173-176.

57. van Velsen EF, Vernooij MW, Vrooman HA, et al. Brain cortical thickness in the general elderly population: the Rotterdam Scan Study. *Neurosci Lett.* 2013;550:189-194.

58. Janowitz D, Wittfeld K, Terock J, et al. Association between waist circumference and gray matter volume in 2344 individuals from two adult community-based samples. *Neuroimage.* 2015;122:149-157.

59. Kharabian Masouleh S, Arelin K, Horstmann A, et al. Higher body mass index in older adults is associated with lower gray matter volume: implications for memory performance. *Neurobiol Aging.* 2016;40:1-10.

60. Jagust W, Harvey D, Mungas D, Haan M. Central obesity and the aging brain. *Arch Neurol.* 2005;62(10):1545-1548.

61. den Heijer T, Vermeer SE, van Dijk EJ, et al. Type 2 diabetes and atrophy of medial temporal lobe structures on brain MRI. *Diabetologia.* 2003;46(12):1604-1610.

62. Korf ES, van Straaten EC, de Leeuw FE, et al. Diabetes mellitus, hypertension and medial temporal lobe atrophy: the LADIS study. *Diabet Med.* 2007;24(2):166-171.

63. Chen X, Wen W, Anstey KJ, Sachdev PS. Effects of cerebrovascular risk factors on gray matter volume in adults aged 60-64 years: a voxel-based morphometric study. *Psychiatry Res.* 2006;147(2-3):105-114.

64. Raz N, Rodrigue KM, Acker JD. Hypertension and the brain: vulnerability of the prefrontal regions and executive functions. *Behav Neurosci.* 2003;117(6):1169-1180.

65. den Heijer T, Hofman A, Koudstaal PJ, Breteler MM. Serum lipids and hippocampal volume: the link to Alzheimer's disease? *Ann Neurol.* 2005;57(5):779-780; author reply 7780.

66. Dearborn JL, Schneider AL, Sharrett AR, et al. Obesity, Insulin Resistance, and Incident Small Vessel Disease on Magnetic Resonance Imaging: Atherosclerosis Risk in Communities Study. *Stroke.* 2015;46(11):3131-3136.

67. Hishikawa N, Yamashita T, Deguchi K, et al. Cognitive and affective functions in diabetic patients associated with diabetes-related factors, white matter abnormality and aging. *Eur J Neurol.* 2015;22(2):313-321.

68. Zhang CE, van Raak EP, Rouhl RP, et al. Metabolic syndrome relates to lacunar stroke without white matter lesions: a study in first-ever lacunar stroke patients. *Cerebrovasc Dis.* 2010;29(5):503-507.

69. Sala M, de Roos A, van den Berg A, et al. Microstructural brain tissue damage in metabolic syndrome. *Diabetes Care.* 2014;37(2):493-500.

70. Tiehuis AM, van der Graaf Y, Visseren FL, et al. Diabetes increases atrophy and vascular lesions on brain MRI in patients with symptomatic arterial disease. *Stroke.* 2008;39(5):1600-1603.

71. Tiehuis AM, van der Graaf Y, Mali WP, et al. Metabolic syndrome, prediabetes, and brain abnormalities on mri in patients with manifest arterial disease: the SMART-MR study. *Diabetes Care.* 2014;37(9):2515-2521.

72. Benedict C, Brooks SJ, Kullberg J, et al. Impaired insulin sensitivity as indexed by the HOMA score is associated with deficits in verbal fluency and temporal lobe gray matter volume in the elderly. *Diabetes Care.* 2012;35(3):488-494.

73. Willette AA, Xu G, Johnson SC, et al. Insulin resistance, brain atrophy, and cognitive performance in late middle-aged adults. *Diabetes Care.* 2013;36(2):443-449.

74. Kotkowski E, Price LR, Franklin C, et al. A neural signature of metabolic syndrome. *Hum Brain Mapp.* 2019.

75. Gerich JE. Control of glycaemia. *Baillieres Clin Endocrinol Metab.* 1993;7(3):551-586.

76. Dimitriadis G, Mitrou P, Lambadiari V, Maratou E, Raptis SA. Insulin effects in muscle and adipose tissue. *Diabetes Res Clin Pract.* 2011;93 Suppl 1:S52-59.

77. Chen C, Cohrs CM, Stertmann J, Bozsak R, Speier S. Human beta cell mass and function in diabetes: Recent advances in knowledge and technologies to understand disease pathogenesis. *Mol Metab.* 2017;6(9):943-957.

78. Cassaglia PA, Hermes SM, Aicher SA, Brooks VL. Insulin acts in the arcuate nucleus to increase lumbar sympathetic nerve activity and baroreflex function in rats. *J Physiol.* 2011;589(Pt 7):1643-1662.

79. Muniyappa R, Iantorno M, Quon MJ. An integrated view of insulin resistance and endothelial dysfunction. *Endocrinol Metab Clin North Am.* 2008;37(3):685-711, ix-x.

80. Shulman GI. Ectopic fat in insulin resistance, dyslipidemia, and cardiometabolic disease. *N Engl J Med.* 2014;371(12):1131-1141.

81. Guilherme A, Virbasius JV, Puri V, Czech MP. Adipocyte dysfunctions linking obesity to insulin resistance and type 2 diabetes. *Nat Rev Mol Cell Biol.* 2008;9(5):367-377.

82. Kullmann S, Heni M, Hallschmid M, Fritsche A, Preissl H, Haring HU. Brain Insulin Resistance at the Crossroads of Metabolic and Cognitive Disorders in Humans. *Physiol Rev.* 2016;96(4):1169-1209.

83. Baura GD, Foster DM, Porte D, Jr., et al. Saturable transport of insulin from plasma into the central nervous system of dogs in vivo. A mechanism for regulated insulin delivery to the brain. *J Clin Invest.* 1993;92(4):1824-1830.

84. Havrankova J, Roth J, Brownstein M. Insulin receptors are widely distributed in the central nervous system of the rat. *Nature.* 1978;272(5656):827-829.

85. Hill JM, Lesniak MA, Pert CB, Roth J. Autoradiographic localization of insulin receptors in rat brain: prominence in olfactory and limbic areas. *Neuroscience.* 1986;17(4):1127-1138.

86. Renner DB, Svitak AL, Gallus NJ, Ericson ME, Frey WH, 2nd, Hanson LR. Intranasal delivery of insulin via the olfactory nerve pathway. *J Pharm Pharmacol.* 2012;64(12):1709-1714.

87. Born J, Lange T, Kern W, McGregor GP, Bickel U, Fehm HL. Sniffing neuropeptides: a transnasal approach to the human brain. *Nat Neurosci.* 2002;5(6):514-516.

88. Fadool DA, Tucker K, Phillips JJ, Simmen JA. Brain insulin receptor causes activity-dependent current suppression in the olfactory bulb through multiple phosphorylation of Kv1.3. *J Neurophysiol.* 2000;83(4):2332-2348.

89. Brunner YF, Benedict C, Freiherr J. Intranasal insulin reduces olfactory sensitivity in normosmic humans. *J Clin Endocrinol Metab.* 2013;98(10):E1626-1630.

90. Ketterer C, Heni M, Thamer C, Herzberg-Schafer SA, Haring HU, Fritsche A. Acute, short-term hyperinsulinemia increases olfactory threshold in healthy subjects. *Int J Obes (Lond).* 2011;35(8):1135-1138.

91. Obici S, Zhang BB, Karkanias G, Rossetti L. Hypothalamic insulin signaling is required for inhibition of glucose production. *Nat Med.* 2002;8(12):1376-1382.

92. Scherer T, O'Hare J, Diggs-Andrews K, et al. Brain insulin controls adipose tissue lipolysis and lipogenesis. *Cell Metab.* 2011;13(2):183-194.

93. Pliquett RU, Fuhrer D, Falk S, Zysset S, von Cramon DY, Stumvoll M. The effects of insulin on the central nervous system--focus on appetite regulation. *Horm Metab Res.* 2006;38(7):442-446.

94. Arnold SE, Arvanitakis Z, Macauley-Rambach SL, et al. Brain insulin resistance in type 2 diabetes and Alzheimer disease: concepts and conundrums. *Nat Rev Neurol.* 2018;14(3):168-181.

95. Nasoohi S, Parveen K, Ishrat T. Metabolic Syndrome, Brain Insulin Resistance, and Alzheimer's Disease: Thioredoxin Interacting Protein (TXNIP) and Inflammasome as Core Amplifiers. *J Alzheimers Dis.* 2018;66(3):857-885.

96. Banks WA, Jaspan JB, Kastin AJ. Effect of diabetes mellitus on the permeability of the blood-brain barrier to insulin. *Peptides.* 1997;18(10):1577-1584.

97. Kaiyala KJ, Prigeon RL, Kahn SE, Woods SC, Schwartz MW. Obesity induced by a high-fat diet is associated with reduced brain insulin transport in dogs. *Diabetes.* 2000;49(9):1525-1533.

98. de la Monte SM. Insulin resistance and Alzheimer's disease. *BMB Rep.* 2009;42(8):475-481.

99. Breteler MM, Stöcker T, Pracht E, Brenner D, Stirnberg R. MRI in the Rhineland study: a novel protocol for population neuroimaging. *Alzheimer's Dement J Alzheimer's Assoc.* 2014;10(4):92.

100. Brenner D, Stirnberg R, Pracht ED, Stocker T. Two-dimensional accelerated MP-RAGE imaging with flexible linear reordering. *MAGMA.* 2014;27(5):455-462.

101. van der Kouwe AJW, Benner T, Salat DH, Fischl B. Brain morphometry with multiecho MPRAGE. *Neuroimage.* 2008;40(2):559-569.

102. Iglesias JE, Augustinack JC, Nguyen K, et al. A computational atlas of the hippocampal formation using ex vivo, ultra-high resolution MRI: Application to adaptive segmentation of in vivo MRI. *Neuroimage.* 2015;115:117-137.

103. Soininen P, Kangas AJ, Wurtz P, Suna T, Ala-Korpela M. Quantitative serum nuclear magnetic resonance metabolomics in cardiovascular epidemiology and genetics. *Circ Cardiovasc Genet.* 2015;8(1):192-206.

104. Matthews DR, Hosker JP, Rudenski AS, Naylor BA, Treacher DF, Turner RC. Homeostasis model assessment: insulin resistance and beta-cell function from fasting plasma glucose and insulin concentrations in man. *Diabetologia.* 1985;28(7):412-419.

105. Hummel T, Konnerth CG, Rosenheim K, Kobal G. Screening of olfactory function with a four-minute odor identification test: reliability, normative data, and investigations in patients with olfactory loss. *Ann Otol Rhinol Laryngol.* 2001;110(10):976-981.

106. Mori K, Nagao H, Yoshihara Y. The olfactory bulb: coding and processing of odor molecule information. *Science.* 1999;286(5440):711-715.

107. Cummings DM, Knab BR, Brunjes PC. Effects of unilateral olfactory deprivation in the developing opossum, Monodelphis domestica. *J Neurobiol.* 1997;33(4):429-438.

108. Korol DL, Brunjes PC. Unilateral naris closure and vascular development in the rat olfactory bulb. *Neuroscience.* 1992;46(3):631-641.

109. Suzuki M, Takashima T, Kadoya M, Takahashi S, Miyayama S, Taira S. MR imaging of olfactory bulbs and tracts. *AJNR Am J Neuroradiol.* 1989;10(5):955-957.

110. Brodoehl S, Klingner C, Volk GF, Bitter T, Witte OW, Redecker C. Decreased olfactory bulb volume in idiopathic Parkinson's disease detected by 3.0-tesla magnetic resonance imaging. *Mov Disord.* 2012;27(8):1019-1025.

111. Hummel T, Urbig A, Huart C, Duprez T, Rombaux P. Volume of olfactory bulb and depth of olfactory sulcus in 378 consecutive patients with olfactory loss. *J Neurol.* 2015;262(4):1046-1051.

112. Yaldizli O, Penner IK, Yonekawa T, et al. The association between olfactory bulb volume, cognitive dysfunction, physical disability and depression in multiple sclerosis. *Eur J Neurol.* 2016;23(3):510-519.

113. Yousem DM, Geckle RJ, Bilker WB, Doty RL. Olfactory bulb and tract and temporal lobe volumes. Normative data across decades. *Ann N Y Acad Sci.* 1998;855:546-555.

114. Wang J, You H, Liu JF, Ni DF, Zhang ZX, Guan J. Association of olfactory bulb volume and olfactory sulcus depth with olfactory function in patients with Parkinson disease. *AJNR Am J Neuroradiol.* 2011;32(4):677-681.

115. Dice LR. Measures of the amount of ecologic association between species. *Ecology.* 1945;26(3):297-302.

116. Burmeister HP, Bitter T, Heiler PM, et al. Imaging of lamination patterns of the adult human olfactory bulb and tract: in vitro comparison of standard- and high-resolution 3T MRI, and MR microscopy at 9.4 T. *Neuroimage.* 2012;60(3):1662-1670.

117. Grundy SM, Cleeman JI, Daniels SR, et al. Diagnosis and management of the metabolic syndrome: an American Heart Association/National Heart, Lung, and Blood Institute Scientific Statement. *Circulation.* 2005;112(17):2735-2752.

118. National Cholesterol Education Program Expert Panel on Detection E, Treatment of High Blood Cholesterol in A. Third Report of the National Cholesterol Education Program (NCEP) Expert Panel on Detection, Evaluation, and Treatment of High Blood Cholesterol in Adults (Adult Treatment Panel III) final report. *Circulation.* 2002;106(25):3143-3421.

119. Team RC. *R: A language and environment for statistical computing.* Vienna, Austria: R Foundation for Statistical Computing; 2017.

120. Bramerson A, Johansson L, Ek L, Nordin S, Bende M. Prevalence of olfactory dysfunction: the skovde population-based study. *Laryngoscope.* 2004;114(4):733-737.

121. Smith W, Murphy C. Epidemiological studies of smell: discussion and perspectives. *Ann N Y Acad Sci.* 2009;1170:569-573.

122. Goektas O, Fleiner F, Sedlmaier B, Bauknecht C. Correlation of olfactory dysfunction of different etiologies in MRI and comparison with subjective and objective olfactometry. *Eur J Radiol.* 2009;71(3):469-473.

123. Assessment of Olfactory Function. In: Hummel T, Welge-Lussen A, eds. *Taste and smell. An Update.* Vol 63. Basel: Karger; 2006:84-98.

124. Doty RL, Smith R, McKeown DA, Raj J. Tests of human olfactory function: principal components analysis suggests that most measure a common source of variance. *Percept Psychophys.* 1994;56(6):701-707.

125. Scuteri A, Laurent S, Cucca F, et al. Metabolic syndrome across Europe: different clusters of risk factors. *Eur J Prev Cardiol.* 2015;22(4):486-491.

126. Carriere I, Peres K, Ancelin ML, et al. Metabolic syndrome and disability: findings from the prospective three-city study. *J Gerontol A Biol Sci Med Sci.* 2014;69(1):79-86.

127. Guallar-Castillon P, Perez RF, Lopez Garcia E, et al. Magnitude and management of metabolic syndrome in Spain in 2008-2010: the ENRICA study. *Rev Esp Cardiol (Engl Ed).* 2014;67(5):367-373.

128. Doty RL, Laing DG. Psychophysical measurement of human olfactory function. In: RL D, ed. *Handbook of olfaction and gustation.* 3rd ed. New York, US: Wiley-Liss; 2015:229-261.

129. Attems J, Walker L, Jellinger KA. Olfactory bulb involvement in neurodegenerative diseases. *Acta Neuropathol.* 2014;127(4):459-475.

130. Gomez C, Brinon JG, Colado MI, et al. Differential effects of unilateral olfactory deprivation on noradrenergic and cholinergic systems in the main olfactory bulb of the rat. *Neuroscience.* 2006;141(4):2117-2128.

131. Mazal PP, Haehner A, Hummel T. Relation of the volume of the olfactory bulb to psychophysical measures of olfactory function. *Eur Arch Otorhinolaryngol.* 2016;273(1):1-7.

132. Servello A, Fioretti A, Gualdi G, et al. Olfactory Dysfunction, Olfactory Bulb Volume and Alzheimer's Disease: Is There a Correlation? A Pilot Study1. *J Alzheimers Dis.* 2015;48(2):395-402.

133. Mugler JP, Brookeman JR. Efficient spatially-selective single-slab 3D Turbo-Spin-Echo Imaging. *Proc Int Soc Magn Reson Med.* 2004;11:695.

134. Kline R. *Principles and practice of structural equation modeling.* 3rd ed. New York, US: Guilford Press; 2011.

135. Hayes AF. *Methodology in the social sciences. Introduction to mediation, moderation, and conditional process analysis: A regression-based approach.* New York, NY, US: Guilford Press; 2013.

136. Rosseel Y. lavaan: An R Package for Structural Equation Modeling. *Journal of Statistical Software.* 2012;48(2):1-36.

137. Vassilaki M, Christianson TJ, Mielke MM, et al. Neuroimaging biomarkers and impaired olfaction in cognitively normal individuals. *Ann Neurol.* 2017;81(6):871-882.

138. Wang J, Eslinger PJ, Smith MB, Yang QX. Functional magnetic resonance imaging study of human olfaction and normal aging. *J Gerontol A Biol Sci Med Sci.* 2005;60(4):510-514.

139. Doty RL. Olfaction in Parkinson's disease and related disorders. *Neurobiol Dis.* 2012;46(3):527-552.

140. Markopoulos F, Rokni D, Gire DH, Murthy VN. Functional properties of cortical feedback projections to the olfactory bulb. *Neuron.* 2012;76(6):1175-1188.

141. Braak H, Braak E. Neuropathological stageing of Alzheimer-related changes. *Acta Neuropathol.* 1991;82(4):239-259.

142. Braak H, Ghebremedhin E, Rub U, Bratzke H, Del Tredici K. Stages in the development of Parkinson's disease-related pathology. *Cell Tissue Res.* 2004;318(1):121-134.

143. Hubbard PS, Esiri MM, Reading M, McShane R, Nagy Z. Alpha-synuclein pathology in the olfactory pathways of dementia patients. *J Anat.* 2007;211(1):117-124.

144. Kovacs T, Cairns NJ, Lantos PL. Olfactory centres in Alzheimer's disease: olfactory bulb is involved in early Braak's stages. *Neuroreport.* 2001;12(2):285-288.

145. Struble RG, Clark HB. Olfactory bulb lesions in Alzheimer's disease. *Neurobiol Aging.* 1992;13(4):469-473.

146. Zapiec B, Dieriks BV, Tan S, Faull RLM, Mombaerts P, Curtis MA. A ventral glomerular deficit in Parkinson's disease revealed by whole olfactory bulb reconstruction. *Brain.* 2017;140(10):2722-2736.

147. Thomann PA, Dos Santos V, Toro P, Schonknecht P, Essig M, Schroder J. Reduced olfactory bulb and tract volume in early Alzheimer's disease--a MRI study. *Neurobiol Aging.* 2009;30(5):838-841.

148. Smitka M, Puschmann S, Buschhueter D, et al. Is there a correlation between hippocampus and amygdala volume and olfactory function in healthy subjects? *Neuroimage.* 2012;59(2):1052-1057.

149. Schubert CR, Cruickshanks KJ, Fischer ME, et al. Olfactory impairment in an adult population: the Beaver Dam Offspring Study. *Chem Senses.* 2012;37(4):325-334.

150. Larsson M, Nilsson LG, Olofsson JK, Nordin S. Demographic and cognitive predictors of cued odor identification: evidence from a population-based study. *Chem Senses.* 2004;29(6):547-554.

151. Doty RL, Cameron EL. Sex differences and reproductive hormone influences on human odor perception. *Physiol Behav.* 2009;97(2):213-228.

152. Seo HS, Guarneros M, Hudson R, et al. Attitudes toward Olfaction: A Cross-regional Study. *Chem Senses.* 2011;36(2):177-187.

153. Dalton P, Doolittle N, Breslin PA. Gender-specific induction of enhanced sensitivity to odors. *Nat Neurosci.* 2002;5(3):199-200.

154. Oliveira-Pinto AV, Santos RM, Coutinho RA, et al. Sexual dimorphism in the human olfactory bulb: females have more neurons and glial cells than males. *PLoS One.* 2014;9(11):e111733.

155. Doty RL, Kamath V. The influences of age on olfaction: a review. *Front Psychol.* 2014;5:20.

156. Lakka HM, Laaksonen DE, Lakka TA, et al. The metabolic syndrome and total and cardiovascular disease mortality in middle-aged men. *JAMA.* 2002;288(21):2709-2716.

157. Wilson PW, D'Agostino RB, Parise H, Sullivan L, Meigs JB. Metabolic syndrome as a precursor of cardiovascular disease and type 2 diabetes mellitus. *Circulation.* 2005;112(20):3066-3072.

158. Eckel RH, Alberti KG, Grundy SM, Zimmet PZ. The metabolic syndrome. *Lancet.* 2010;375(9710):181-183.

159. Friedman JI, Tang CY, de Haas HJ, et al. Brain imaging changes associated with risk factors for cardiovascular and cerebrovascular disease in asymptomatic patients. *JACC Cardiovasc Imaging.* 2014;7(10):1039-1053.

160. Beauchet O, Celle S, Roche F, et al. Blood pressure levels and brain volume reduction: a systematic review and meta-analysis. *J Hypertens.* 2013;31(8):1502-1516.

161. Kotkowski E, Price LR, Franklin C, et al. A neural signature of metabolic syndrome. *Hum Brain Mapp.* 2019;40(12):3575-3588.

162. Hermans MP, Levy JC, Morris RJ, Turner RC. Comparison of tests of beta-cell function across a range of glucose tolerance from normal to diabetes. *Diabetes.* 1999;48(9):1779-1786.

163. Fischl B. FreeSurfer. *Neuroimage.* 2012;62(2):774-781.

164. Benjamini Y, Krieger AM, Yekutieli D. Adaptive linear step-up procedures that control the false discovery rate. *Biometrika.* 2006(93):491-507.

165. Klein A, Tourville J. 101 labeled brain images and a consistent human cortical labeling protocol. *Front Neurosci.* 2012;6:171.

166. Akintola AA, van den Berg A, Altmann-Schneider I, et al. Parameters of glucose metabolism and the aging brain: a magnetization transfer imaging study of brain macro- and micro-structure in older adults without diabetes. *Age (Dordr).* 2015;37(4):9802.

167. Young SE, Mainous AG, 3rd, Carnemolla M. Hyperinsulinemia and cognitive decline in a middle-aged cohort. *Diabetes Care.* 2006;29(12):2688-2693.

168. Seo M, Lee YS, Moon SS. Association of hearing impairment with insulin resistance, beta-cell dysfunction and impaired fasting glucose before onset of diabetes. *Diabet Med.* 2016;33(9):1275-1282.

169. Poh S, Mohamed Abdul RB, Lamoureux EL, Wong TY, Sabanayagam C. Metabolic syndrome and eye diseases. *Diabetes Res Clin Pract.* 2016;113:86-100.

170. Lin F, Lo RY, Cole D, et al. Longitudinal effects of metabolic syndrome on Alzheimer and vascular related brain pathology. *Dement Geriatr Cogn Dis Extra.* 2014;4(2):184-194.

171. Lotsch J, Hummel T. A machine-learned analysis suggests non-redundant diagnostic information in olfactory subtests. *IBRO Rep.* 2019;6:64-73.

172. Ramaekers MG, Boesveldt S, Lakemond CM, van Boekel MA, Luning PA. Odors: appetizing or satiating? Development of appetite during odor exposure over time. *Int J Obes (Lond).* 2014;38(5):650-656.

173. Zoon HF, de Graaf C, Boesveldt S. Food Odours Direct Specific Appetite. *Foods.* 2016;5(1).

174. Chen Y, Lin YC, Kuo TW, Knight ZA. Sensory detection of food rapidly modulates arcuate feeding circuits. *Cell.* 2015;160(5):829-841.

175. Betley JN, Xu S, Cao ZFH, et al. Neurons for hunger and thirst transmit a negative-valence teaching signal. *Nature.* 2015;521(7551):180-185.

176. Nederkoorn C, Smulders FT, Jansen A. Cephalic phase responses, craving and food intake in normal subjects. *Appetite.* 2000;35(1):45-55.

177. Johnson WG, Wildman HE. Influence of external and covert food stimuli on insulin secretion in obese and normal persons. *Behav Neurosci.* 1983;97(6):1025-1028.

178. Teff KL, Mattes RD, Engelman K. Cephalic phase insulin release in normal weight males: verification and reliability. *Am J Physiol.* 1991;261(4 Pt 1):E430-436.

179. Zoon HF, He W, de Wijk RA, de Graaf C, Boesveldt S. Food preference and intake in response to ambient odours in overweight and normal-weight females. *Physiol Behav.* 2014;133:190-196.

180. Ferriday D, Brunstrom JM. How does food-cue exposure lead to larger meal sizes? *Br J Nutr.* 2008;100(6):1325-1332.

181. Ferriday D, Brunstrom JM. 'I just can't help myself': effects of food-cue exposure in overweight and lean individuals. *Int J Obes (Lond).* 2011;35(1):142-149.

182. McGann JP. Poor human olfaction is a 19th-century myth. *Science.* 2017;356(6338).

11. Acknowledgement

This dissertation would never have been possible without the encouragement, dedication, and support of a number of people.

First and foremost, I would like to express my deepest gratitude to my supervisor, Prof. Dr. Dr. Monique M. B. Breteler, for her patience and continuous guidance and support throughout my PhD. Her constructive comments have greatly enriched my knowledge and helped me develop my research.

Besides my supervisor, I would also like to thank the rest of my thesis committee members: Prof. Dr. Aad van de Lugt, Prof. Dr. Elke Hattingen, and Prof. Dr. Henning Boecker for their encouragement, and invaluable comments and suggestions.

Sincere thanks would go to Dr. Ahmad Aziz, who was always willing to provide his great insights, and constantly help me in writing.

I would like to express my appreciation to the entire group of the Rhineland Study, for their friendship, enthusiasm, expertise, as well as prompt help whenever I needed it. I really enjoyed the time with them. I would also thank all the participants in the study for providing the data.

Special mention goes to Prof. Dr. Martin Reuter and his team, especially Kersten Diers, for their unfailing assistance in the analysis.

I gratefully acknowledge the financial support from China Scholarship Council.

Last but not least, I am indebted to my friends and family for their continuous and unconditional support, which keeps me going when times were tough.